Numerical simulations of astrophysical black-hole binaries

Habilitationsschrift

zur Erlangung des akademischen Grades
doctor rerum naturalium habilitatus (Dr. rer. nat. habil.)

vorgelegt dem Rat der
Physikalisch-Astronomisch-Technikwissenschaftlichen Fakultät
der Friedrich-Schiller-Universität Jena

von Dr. phil. Ulrich Sperhake
geboren am 14. April 1968 in Buchholz i. d. Nordheide

Gutachter

1.

2.

3.

Tag der öffentlichen Verteidigung:

Tag des öffentlichen Vortrages (Lehrprobe):

Chapter 1

Introduction

It is probably not an exaggeration to rate the development of quantum theory and general relativity in the early twentieth century among mankind's most remarkable achievements. The conceptual ideas employed therein to successfully model natural phenomena are so alien to human day-to-day experience that the theories' influence has gone beyond the realm of scientific application and also touched some of our most profound philosophical ideas. Among the most bizarre concepts introduced by quantum theory and relativity we find the uertainty principle, superposition and reduction of states, the big bang and black holes. It is the physical properties of black-hole-binary systems and their role in contemporary research in the areas of fundamental physics, astrophysics and gravitational wave physics which forms the subject of the present thesis.

Black holes are predicted by Einstein's theory of general relativity. According to the singularity theorems of Hawking and Penrose [167, 166], spacetime singularities are an inevitable consequence if one makes minimal assumptions on the matter-energy present in the spacetime. By implication of the cosmic censorship conjecture, singularities must be causally disconnected from the exterior spacetime via an event horizon which represents the fundamental definition of a black hole. The singular nature of black holes adds an even more bizarre feature to the theory of general relativity: by construction, general relativity is not valid at singular points and thus predicts its own incompleteness as a physical theory. Indeed, it is generally accepted, that a unified theory of quantum gravity will overcome the pathologies encountered at spacetime singularities. In spite of intense research efforts, however, such a combination of general relativity and quantum mechanics is currently not available.

From the viewpoint of differential geometry, black holes are regions of spacetime where the curvature prevents light rays from escaping towards null infinity, i. e. regions which are causally disconnected from their surroundings. Spacetime curvature is a fundamental concept of Einstein's theory of general relativity, as gravitation is a manifestation of this curvature rather than a force in the traditional sense. The basic quantity which encapsulates all information about the spacetime curvature is the metric, a set of ten functions of space and time coordinates. This metric obeys the Einstein equations which equates the Einstein tensor, a complex combination of the metric and its first and second derivatives, with the mass-energy tensor describing the matter distribution. The Einstein equations thus represent a system of ten second order partial differential equations, one of the most complicated systems of equations in all of physics. Einstein himself did not expect physically meaningful solutions to be found analytically and it came as a surprise when Karl Schwarzschild found his famous solution of a static, spherically symmetric vacuum spacetime just a few months after the publication of general relativity in 1916. This solution is now known as a "Schwarzschild black hole", but the term black hole was not coined until much later by John Wheeler. The Schwarzschild solution has led to invaluable insight into general relativity and was soon generalized to include electric charge in the form of the Reisner-Nordström solution. The key simplification leading to these analytic solutions is the high degree of symmetry of the spacetime which reduces the Einstein equations to a one-dimensional problem with no time dependence. Relaxing the assumption of spherical symmetry to allow for a spacetime with non-vanishing angular momentum led to a much more complex system of equations even in the limit of stationarity. It took more than four decades until Roy Kerr found the analytic expressions for the metric of an axisymmetric spacetime containing a rotating black hole [183]. Again, the inclusion of electric charge resulted in a generalization, the so-called Kerr-Newman solution.

For a long time, these black hole solutions were considered a mathematical feature rather than objects of physical relevance. This picture has changed dramatically in the course of recent decades, however. Not only are black holes now accepted as a common end product of the evolution of very massive stars, they are also recognized as almost ubiquitously present in the form on super-massive black holes (SMBH) at the centers of at least more massive galaxies [193]. The formation history of these SMBHs is subject of ongoing research in astrophysics and is likely to be closely interrelated with structure formation in the universe in general (see e. g. [126, 160, 293, 159, 209, 210, 295, 200, 294]). Observations of the central regions of galaxies have also revealed significant correlation of the masses of black holes with the structure of the galaxy cores, specifically the velocity dispersions and the density profiles [131, 145, 218, 223, 75, 219]. Given the all absorbing nature of black holes, it is quite remarkable, that they also form the engine for the strongest sources of electromagnetic radiation observed in the universe. Active galactic nuclei are now commonly believed to be driven by accretion around black holes. Their observation at cosmological redshifts provides valuable constraints on the formation history of SMBHs. Most notably, the discovery of the most luminous quasar at $z \approx 6$ in the Sloan Digital Sky Survey [129] implies that black holes of masses around $10^9\ M_\odot$ were already in existence less than 10^9 years after the big bang.

Black holes also play a fundamental role in the ongoing effort to detect gravitational waves. This type of radiation is general relativity's analogue of electromagnetic waves and is a direct consequence of the Einstein equations. In fact, such radiative solutions were recognized by Einstein himself, but were subject of a long-lasting debate on whether they represent gauge effects or truly physical phenomena. There is no doubt left on the physical nature of gravitational waves (GW) now, but their direct detection is made enormously difficult by their extremely weak interaction with matter. To date, therefore, the only evidence for the existence of gravitational waves is indirect and based on observations of binary pulsar systems. Most notably, decade long observations of the Hulse-Taylor pulsar 1913+16 show a gradual decrease in the orbital period which is in excellent agreement with the energy loss of the system expected from emission of gravitational waves according to the theory of general relativity [177, 284]. This indirect evidence has led to the award of the 1993 Nobel Prize to Hulse and Taylor and also provided motivation for the construction of laser interferometric detectors in multi-national collaborations such as the American LIGO [6, 125], the European GEO600 [207] and VIRGO [53, 9] and the Japanese TAMA [283, 20]. A space based interferometer, LISA [168], is targeted for launch in 2018 and will facilitate high signal-to-noise ratio measurements of low-frequency gravitational wave sources. The strongest source for all these detectors is the inspiral and coalescence of black hole binaries. Obtaining a detailed theoretical understanding of these binary systems is crucial to support the effort to directly detect GWs.

The enormous complexity of the Einstein equations in the absence of strong symmetry and/or time independence makes it impossible to study binary black hole systems analytically in the framework of full general relativity. In consequence, the theoretical modeling has pursued two alternative approaches. The first replaces general relativity by an approximative description of the physics which allow for analytic studies. In particular, binaries can be described with good accuracy in the framework of post-Newtonian (PN) theory as long as they orbit each other with sufficient separation (see [61] for a review). In the late stages after the merger of the binary, in contrast, the system closely resembles a single Kerr hole and is described well by perturbation theory, i. e. the linearization of Einstein's equations around a Kerr background. We will return to both of these approximation theories below. The second approach to studying binary systems is to use numerical methods to solve the full Einstein equations. The research field concerned with this approach is called numerical relativity and is the main subject of this work.

It is a remarkable coincidence that major breakthroughs in numerical relativity have been achieved at almost exactly the same time that the above mentioned ground-based laser interferometers have advanced to the stage that they are capable of performing observation runs at or close to the design sensitivity. These are therefore very exciting times for black-hole and gravitational-wave physics and the community is about to open an entirely new window to the universe with unprecedented opportunities to gain fundamentally new insight into the structure and evolution of the universe.

The main purpose of Chapters 1-7 of this work is to provide the context for the published articles which form the core of this thesis. For this purpose, we summarize in Chapter 2 the 3+1 decomposition of spacetime. A list of ingredients for a numerical simulation is given in Chapter 3. Methods to extract physical information from a simulation are discussed in Chapter 4. In Chapters 5 and 6, we present a brief overview of the history of black hole simulations and summarize results obtained in the last few years following the breakthrough in binary simulations in 2005. We conclude with the set of published scientific articles which form the core of this work.

Notation: We use geometric units, that is we set the gravitational constant G and the speed of light c to unity. We use Einstein summation, that is repeated indices represent implicit summations, as for example in

$$T^{\alpha}{}_{\mu}n^{\mu} \equiv \sum_{\mu=0}^{3} T^{\alpha}{}_{\mu}n^{\mu}. \tag{1.1}$$

Specifically, Latin indices run from 1 to 3 and Greek indices from 0 to 3. In sign convention we follow [148] and use the convention of Misner, Thorne and Wheeler [226].

Chapter 2

The "3+1" decomposition of general relativity

The numerical solution of the Einstein equations faces a multitude of conceptual difficulties commonly not present in other areas of computational physics. We will discuss various of these problems further below, but we cannot even get started without addressing the most fundamental problem; the Einstein equations are expressed in terms of geometrical objects, so-called tensors. Computers, in contrast, exclusively operate on numbers. The first step in translating the Einstein equations into a form digestible for a numerical treatment is therefore to use a basis expansion and consider the components of the equations $G_{\alpha\beta} = 8\pi T_{\alpha\beta}$, where G and T are the Einstein and matter tensor to be discussed in more detail below. The components of any tensor can be represented in the form of arrays on discrete numerical grids. There still remains the question of the hyperbolic, parabolic and/or elliptic nature of the Einstein equations. The former two typically describe physical systems as the time evolution of the state, the latter in the form of equilibrium configurations.

The most common approach to disentangle the nature of the Einstein equations is the so-called "3+1" decomposition based on the canonical work of Arnowitt, Deser and Misner (ADM) [30] and later formulated by York [302, 303]. The result is a combined hyperbolic-elliptic systems, that is, the equations separate into a set of evolution equations plus some constraints.

The key idea in this procedure is to decompose the four-dimensional spacetime into a one-parameter family of three-dimensional spatial slices. Each of these slices describes a snapshot of the system under consideration and the Einstein equations tell us how the system evolves from one snapshot to the next. Each slice is described in terms of the components of two fundamental tensors or "forms", the spatial three-metric and the extrinsic curvature. In practice, one evolves the components of these tensors and we need a basis expansion to assign unique meaning to these fields of numbers. Commonly this basis is a coordinate basis, so that our remaining task is to specify the coordinates. The physics of the system can only be interpreted as a combination of the tensor components (their numerical values) with the meaning of the coordinates. While the choice of coordinates is in principle arbitrary because of the covariance of general relativity, the actual choice of coordinates turns out to be crucial for obtaining a stable numerical scheme. We will discuss this issue in more detail below.

In this thesis, we focus on numerical work based on the 3+1 decomposition. We emphasize, however, that alternative approaches have been investigated. The most important alternative is based on the characteristics of the Einstein equations, the light or null cones. These characteristic or null foliations of spacetime have been pioneered in the seminal work of Bondi and Sachs [69, 258] and lead to a remarkably simple hierarchy of the Einstein equations. The main difficulty of the characteristic approach is the break-down of the characteristic coordinate systems in regions of strong curvature due to the formation of caustics. The characteristic approach is still subject of considerable research and has also inspired the combined use with 3+1 or Cauchy formulations of general relativity in the form of Cauchy-characteristic matching. For further details the reader is referred to the review articles [198, 297] and references therein.

An alternative combination of the benefits of the 3+1 and characteristic decomposition can be obtained using the conformal field equations based on the studies by Friedrich [137]. Here one evolves hyperboloidal surfaces which are spatial everywhere but asymptote towards null infinity. More information about this approach can be found in Frauendiener's review article [136] as well as references therein.

We conclude this introduction by pointing to further review articles on numerical relativity and black hole simulations. All the items mentioned above are summarized in the article by Lehner [198]. A comprehensive summary including a detailed description of the “3+1” formulation in lecture-style format is given in Gourgoulhon's review article [148]. A review focusing more on the mathematical aspects of numerical relativity and the relationship between numerical and mathematical relativity is given in Jaramillo *et al.* [182]. More details on the numerical techniques used for modeling compact binaries including a more in-depth discussion of neutron stars is given by Baumgarte and Shapiro [52]. The most recent review article by Pretorius [252] summarizes results of black hole simulations performed after the breakthroughs of 2005 with particular emphasis on the final stages of the coalescence.

Because of its conceptual importance for the remainder of the present thesis, we now address in more detail the "3+1" decomposition of the spacetime manifold and the Einstein equations.

2.1 The Einstein equations

The fundamental quantity which we need to determine is the four-dimensional spacetime metric $g_{\alpha\beta}$. As the metric is a symmetric tensor, this corresponds to ten independent components. Once we know the metric, we can calculate the Christoffel connection

$$\Gamma^{\alpha}_{\beta\gamma} = \frac{1}{2} g^{\mu\alpha} \left(\partial_\beta g_{\gamma\mu} + \partial_\gamma g_{\mu\beta} - \partial_\mu g_{\beta\gamma} \right), \tag{2.1}$$

where $g^{\alpha\beta}$ is the inverse of the metric. From the connection we obtain the covariant derivative

$$\nabla_\alpha T^{\beta\ldots}{}_{\rho\ldots} \equiv \partial_\alpha T^{\beta\ldots}{}_{\rho\ldots} + \Gamma^{\beta}_{\mu\alpha} T^{\mu\ldots}{}_{\rho\ldots} + \ldots \quad - \Gamma^{\mu}_{\rho\alpha} T^{\beta\ldots}{}_{\mu\ldots} - \ldots \quad , \tag{2.2}$$

with corresponding additional terms for each further index of T, and the Riemann tensor

$$R^{\alpha}{}_{\beta\gamma\delta} = \partial_\gamma \Gamma^{\alpha}_{\beta\delta} - \partial_\delta \Gamma^{\alpha}_{\beta\gamma} + \Gamma^{\alpha}_{\mu\gamma} \Gamma^{\mu}_{\beta\delta} - \Gamma^{\alpha}_{\mu\delta} \Gamma^{\mu}_{\beta\gamma}. \tag{2.3}$$

We thus have all the information to compute geodesics in this spacetime, geodesic deviation and, as we will see below, the total mass and the gravitational radiation generated in the spacetime.

In order to determine the metric, we need to solve the Einstein equations

$$G_{\alpha\beta} \equiv R_{\alpha\beta} - \frac{1}{2} R g_{\alpha\beta} = T_{\alpha\beta}, \tag{2.4}$$

where the Ricci tensor and scalar are defined as contractions of the Riemann tensor: $R_{\beta\delta} = R^{\mu}{}_{\beta\mu\delta}$ and $R = R^{\mu}{}_{\mu}$. The matter energy tensor $T_{\alpha\beta}$ describes the matter distribution of the spacetime.

Finding solutions to the Einstein equations is actually a simple task. Just take any metric, compute the Riemann tensor according to Eq. (2.3), calculate the Ricci tensor and scalar and finally the matter tensor $T_{\alpha\beta}$ from Eq. (2.4). This provides a solution to the Einstein equations with the matter sources $T_{\alpha\beta}$. The problem with this approach is that matter tensors calculated in this way will in general not correspond to any physically meaningful or realistic matter distribution. The difficult part is therefore not finding solutions to the Einstein equations, but rather finding physically meaningful solutions. This is also the remarkable feature of the Schwarzschild and Kerr solutions. They represent meaningful solutions, now believed to closely resemble real, existing, physical objects. We therefore need to first prescribe the energy matter tensor $T_{\alpha\beta}$ and then determine the metric from the system of partial differential equations (2.4).

Black holes are vacuum solutions to the Einstein equations and as such obey the vacuum Einstein equations which can be written as

$$R_{\alpha\beta} = 0. \tag{2.5}$$

In the remainder of this work we will exclusively study systems with vanishing energy matter tensor $T_{\alpha\beta} = 0$. We do not abandon the energy matter tensor, however, without emphasizing that the simulation of compact binaries involving neutron stars has been subject to comparable numerical efforts as has been the study of black-hole binaries. Indeed, the first orbital simulations of compact binaries to have been achieved in numerical relativity were neutron-star-binary evolutions [269, 212, 222]. For more details and recent developments of neutron-star, mixed black-hole-neutron-star as well as boson-star binaries, the reader is referred to these papers as well as [52, 237, 19, 268, 128] and references therein.

As a starting point for the 3+1 decomposition we consider a four-dimensional manifold $\mathcal{M}$ with coordinates x^α and a metric of signature $- + + +$. We next require a foliation. That is, we assume that there exists a function $t(x^\alpha)$ of the spacetime coordinates x^α with non-vanishing gradient everywhere. Without loss of generality we assume the the gradient satisfies $g_{\mu\nu}\nabla^\mu t \nabla^\nu t < 0$. In consequence, the slices $t = \text{const}$ are spacelike in the sense that the norm of any vector tangent to the slices is positive, i. e. has the opposite sign of the norm of ∇t. The foliation is graphically illustrated in Fig. 2.1 where we show two hypersurfaces corresponding to $t = 0$ and $t = dt$. We next consider vectors v tangent to a hypersurface Σ_t with fixed t. By definition these vectors have vanishing inner product with the gradient of t: $v^\mu \nabla_\mu t = 0$. The timelike normal field of the hypersurfaces is therefore given by

$$n_\alpha = \frac{\nabla_\alpha t}{\sqrt{-\nabla^\mu t \nabla_\mu t}}, \tag{2.6}$$

and its dual vector field is $n^\alpha = g^{\alpha\mu} n_\mu$.

It turns out to be convenient to use coordinates adapted to the 3+1 foliation. These are given by t and three further coordinates labeling points inside each hypersurface Σ_t. These spatial coordinates x^i define a three-parameter family of curves

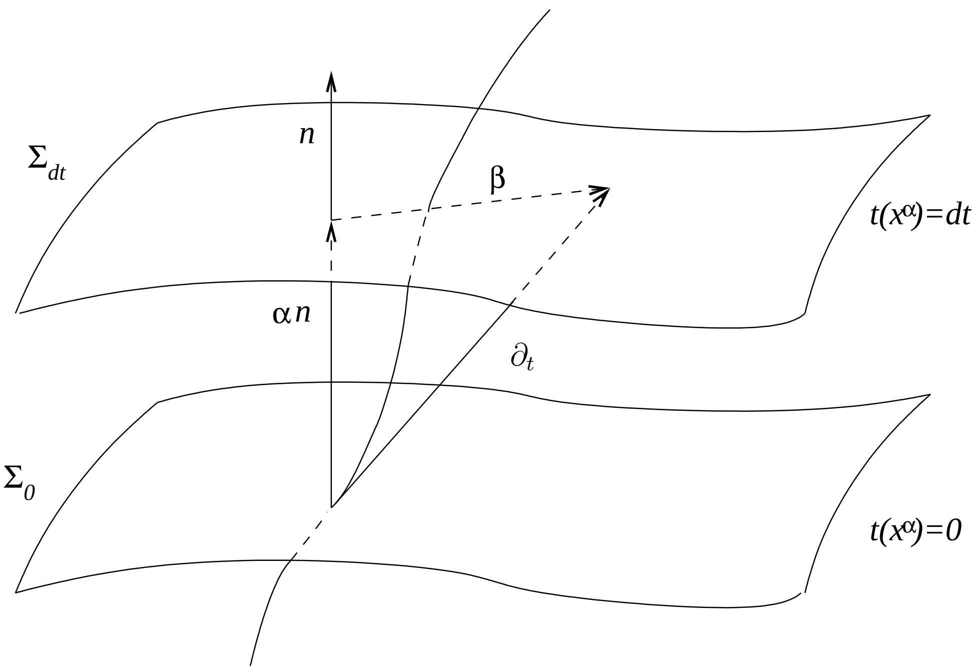

Figure 2.1: Illustration of a timelike foliation of spacetime. One spatial dimension is suppressed for presentation purposes.

x^i = const which thread the foliation, that is, any such curve intersects each hypersurface Σ_t exactly once. In Fig. 2.1 we have illustrated such a curve together with its tangent vector ∂_t. We emphasize that ∂_t is in general not orthogonal to the hypersurfaces Σ_t.

We have now split the coordinate freedom into two different parts. First, we can choose the foliation via the function t, second we have the freedom to label the points inside any hypersurface by choosing the spatial coordinates x^i. In the majority of formulations of the Einstein equations, this freedom is encapsulated in the following two functions. First, the lapse function is defined as

$$\alpha = \sqrt{-\nabla^\mu t \nabla_\mu t}. \tag{2.7}$$

Loosely speaking, it represents a measure for the separation in proper time between two neighboring hypersurfaces Σ_t and Σ_{t+dt}. Translated into a more numerical language, the lapse function enables us to control the advance in proper time corresponding to an advance in coordinate time dt. Often, one wants to slow down the advance in proper time in regions where the code encounters a singularity by locally decreasing the lapse towards zero.

The second gauge function is the shift vector defined by

$$\beta^i = (\partial_t)^i - \alpha n^i. \tag{2.8}$$

as illustrated in Fig. 2.1. The shift vector determines how points with identical spatial labels x^i are identified on neighboring slices.

Given the decomposition of spacetime into a timelike foliation of spacelike slices, it will be helpful to apply a similar decomposition to the geometric objects. For this purpose we define the projection operator

$$\perp^\mu{}_\alpha = \delta^\mu{}_\alpha + n^\mu n_\alpha. \tag{2.9}$$

For any given tensor this enables us to define its spatial projection. For example, for a tensor $T^\alpha{}_\beta$ we have

$$\perp T^\alpha{}_\beta = \perp^\alpha{}_\mu \perp^\nu{}_\beta T^\mu{}_\nu, \tag{2.10}$$

and likewise for tensors with different arrangements of indices. Projections onto the time direction are directly obtained from contraction with the unit normal field n^α. For our example we obtain the time projection $T^\mu{}_\nu n_\mu n^\nu$. We can also define mixed projections, as for example $\perp^\alpha{}_\mu T^\mu{}_\nu n^\nu$.

In particular, we can apply the projection operator to the metric itself and obtain

$$\gamma_{\alpha\beta} \equiv \perp g_{\alpha\beta} = g_{\alpha\beta} + n_\alpha n_\beta = \perp_{\alpha\beta}. \tag{2.11}$$

This projection of the metric defines an induced three-dimensional metric on the hypersurface in the sense that its effect on all geometric objects tangent to the hypersurface is the same as if the spacetime metric were acting on them, and its contraction with objects orthogonal to the hypersurface vanish.

We now recall the definitions of the connection and the Riemann tensor in Eqs. (2.1) and (2.3). These definitions are valid for an arbitrary dimension and thus also apply to the induced metric. We merely replace Greek with Latin indices in these definitions and obtain the three-dimensional Christoffel connection and Riemann tensor. From the connection we derive the three-dimensional covariant derivative D_a. For example, for a three-dimensional tensor with one upper and one lower index, the covariant derivative is

$$D_a T^b{}_c = \partial_a T^b{}_c + \Gamma^b_{ia} T^i{}_c - \Gamma^i_{ca} T^b{}_i. \tag{2.12}$$

If we use coordinates adapted to the 3+1 decomposition, this can be shown to be identical to the spatial components of

$$D_\alpha T^\beta{}_\gamma = \perp^\alpha{}_\mu \perp^\beta{}_\nu \perp^\rho{}_\gamma \nabla_\mu T^\nu{}_\rho. \tag{2.13}$$

In summary, we can apply the entire machinery of differential geometry to the induced three-metric $\gamma_{\alpha\beta}$ just as we applied it to the four-metric $g_{\alpha\beta}$. We still need to work out, however, how these three-dimensional objects are related to their four-dimensional counterparts.

Before we address this question, though, we need to introduce the extrinsic curvature which is defined as

$$K_{\alpha\beta} = -\perp^\mu{}_\alpha \perp^\nu{}_\beta \nabla_\nu n_\mu. \tag{2.14}$$

As illustrated in Figs. 2.2-2.4 of Ref. [148], the extrinsic curvature can be interpreted as the variation of the timelike unit normal field on the hypersurface. We emphasize that $K_{\alpha\beta}$ is by definition a purely spatial quantity. A straightforward calculation leads to the important equivalent relation

$$K_{\alpha\beta} = -\frac{1}{2}\mathcal{L}_n \gamma_{\alpha\beta}, \tag{2.15}$$

where $\mathcal{L}_n$ is the Lie-derivative along the unit normal field n^α.

We next address the question of how the four-dimensional Riemann tensor is related to the three-dimensional quantities. This is best done by considering the projections of the four-dimensional Riemann tensor. The calculations are lengthy but straightforward and the interested reader is referred to [148]. Here we merely list the resulting relations

$$\begin{aligned}
\perp^\mu{}_\alpha \perp^\nu{}_\beta \perp^\gamma{}_\rho \perp^\sigma{}_\delta R^\rho{}_{\sigma\mu\nu} &= \mathcal{R}^\gamma{}_{\delta\alpha\beta} + K^\gamma{}_\alpha K_{\delta\beta} - K^\gamma{}_\beta K_{\alpha\delta}, && (2.16)\\
\perp^\mu{}_\alpha \perp^\nu{}_\beta \perp^\gamma{}_\rho n^\sigma R^\gamma{}_{\sigma\alpha\beta} &= D_\beta K^\gamma{}_\alpha - D_\alpha K^\gamma{}_\beta, && (2.17)\\
\perp_{\rho\alpha} \perp^\mu{}_\beta n^\sigma n^\nu R^\rho{}_{\sigma\mu\nu} &= \mathcal{L}_n K_{\alpha\beta} + \frac{1}{\alpha} D_\alpha D_\beta \alpha + K_{\alpha\mu} K^\mu{}_\beta, && (2.18)
\end{aligned}$$

where we use the symbol $\mathcal{R}$ to distinguish the three-dimensional Riemann tensor from its four-dimensional counterpart R. These equations are often referred to as the Gauss-Codacci or Gauss-Codacci-Mainardi equations. We note that all further projections vanish due to the symmetry of the Riemann tensor. Contracted versions of these equations are straightforwardly obtained by multiplication with the metric $g^{\alpha\beta}$.

If we look at the right hand sides of these relations, all terms except for the Lie derivative of $K_{\alpha\beta}$ are purely spatial expressions. In adapted coordinates (t, x^i) we are therefore allowed to replace Greek by Latin indices which run from 1 to 3 only. The Lie derivative of the extrinsic curvature, on the other hand, can be rewritten as

$$\mathcal{L}_n K_{\alpha\beta} = \mathcal{L}_{\frac{1}{\alpha}(\partial_t - \beta)} K_{\alpha\beta} = \frac{1}{\alpha}\left(\mathcal{L}_{\partial_t} - \mathcal{L}_\beta\right) K_{\alpha\beta} = \frac{1}{\alpha}\left(\partial_t K_{\alpha\beta} - \mathcal{L}_\beta\right) K_{\alpha\beta}, \tag{2.19}$$

where the Lie derivative of the extrinsic curvature along the shift vector β is again a purely spatial quantity.

Finally, we are in the position to decompose the Einstein equations $R_{\alpha\beta} = 0$ themselves. Again we refer the reader for details of the calculations to [148] and summarize the results. As with the Riemann tensor, there are three projections. First, we can project both indices onto the time direction. Inserting the above projections of the Riemann tensor into $R_{\mu\nu} n^\mu n^\nu$ leads to

$$\mathcal{H} \equiv \mathcal{R} + K^2 - K_{mn} K^{mn} = 0 \tag{2.20}$$

where $K = \gamma^{mn} K_{mn}$ is the trace of the extrinsic curvature. This equation is known as the Hamiltonian constraint. It does not contain any time derivatives but instead is a relation which must be obeyed by the three-metric γ_{ij} and the extrinsic curvature K_{ij} on each hypersurface. Similarly, we obtain the momentum constraint from the mixed projection $\perp R_{\alpha\mu} n^\mu$

$$\mathcal{M}^i \equiv D^i K - D_m K^{im} = 0 \tag{2.21}$$

All the information about the time evolution is contained in the spatial projection $\perp R_{\alpha\beta} = 0$ which leads to

$$(\partial_t - \mathcal{L}_\beta) K_{ij} = -D_i D_j \alpha + \alpha\left(\mathcal{R}_{ij} - 2K_{im} K^m{}_j + K_{ij} K\right). \tag{2.22}$$

Together with Eq. (2.15), this equation forms a second order in time evolution system for the induced metric γ_{ij}. This system together with the Hamiltonian and momentum constraints are often referred to as the "ADM" equations. This term is not strictly correct because Arnowitt, Deser and Misner used the canonical momenta in place of the extrinsic curvature in their original work [30]. We will follow common notation here, however, and will talk of the ADM equations in the remainder of this work.

It is this set of equations which is at the heart of the majority of work in numerical relativity. It is highly instructive to discuss these equations in more detail. First, we note that the equations do not provide any information on the gauge functions α and β^i. This is expected as these functions incorporate the coordinate freedom of general relativity and therefore can be specified arbitrarily. Second, we count the degrees of freedom. We have a second order system in time for the six independent components of the symmetric three-metric γ_{ij}. Four of these are determined by the constraints, so that there remain two dynamic degrees of freedom, the two degrees of freedom of gravitation. Finally, the Bianchi identities

$$\nabla_\nu R^\alpha{}_{\beta\lambda\mu} = 0, \qquad \nabla_\nu G^{\mu\nu} = 0, \tag{2.23}$$

can be shown to propagate the constraint equations through the evolution. That is, if the constraints are satisfied on some initial hypersurface and the evolution equations hold, then the constraints are automatically satisfied on all other hypersurfaces. This greatly simplifies the task of numerically evolving data; it is sufficient to enforce the constraints on the initial data and evolve these using Eqs. (2.15) and (2.22).

In summary, we have reformulated the Einstein equations as an initial value problem. Given an initial snapshot of the three-metric γ_{ij} and the extrinsic curvature K_{ij}, we merely need to specify gauge functions α and β^i and subsequently can evolve the data and reconstruct the entire spacetime. It is this conceptual simplicity of numerical relativity that has inspired the community with a great deal of optimism following the early work in the 1970s. In the next section, we will discuss the difficulties which have prevented the community from successfully implementing the above recipe for several decades and also the solutions which finally have resulted in the breakthroughs of 2005.

Chapter 3

The ingredients of numerical relativity

3.1 The formulation of the Einstein equations

We have discussed in detail how the ADM equations provide a conceptually simple recipe for evolving a given set of initial data using numerical methods in general relativity. Unfortunately, all attempts of implementing these equations have resulted in numerical instabilities after timescales much shorter than the dynamical timescale of the systems under consideration. Because of their enormous complexity, the evolution equations defy all attempts of directly applying standard stability analysis. Most likely, the instabilities observed in numerical relativity for such a long time are a consequence of various causes. It is now commonly believed, however, that the structure of the ADM equations makes them an unlikely candidate for providing long-term stable numerical evolutions.

The key difficulty here is that the Einstein equations are a constrained system. We have seen above, how the Einstein equations can be decomposed into evolution equations and constraints. This decomposition is not unique, however. For example, we can add any combination of the constraints to the right hand side of the evolution equations and thus obtain a different system. All such decompositions describe the same physics and will have identical physical (constraint satisfying) solutions. But the evolution equations also admit non-physical (constraint violating) solutions and this unphysical solution space depends on the decomposition. In particular, some decompositions will allow for unphysical solutions which rapidly grow beyond control. We need to bear in mind in this context that any numerical solution will inevitably satisfy the constraints only within some accuracy, so that such rapidly growing solutions, if present, are likely to be excited by numerical noise. It is desirable, for this purpose, to have a smooth dependence of the space-time solution on the initial data. This quality is encapsulated in the well-posedness of the system of equations. While a well-posed system does not guarantee stable numerical evolutions, it is generally accepted that a well-posed evolution system is a much more likely candidate for successful numerical simulations.

The common approach to obtain well-posedness and thus some bounds on the deviation in the time evolution of neighboring initial data sets is based on using strongly or symmetric hyperbolic systems (see e. g. [155] and references therein for definitions). Indeed, it has been shown in [188] that a first order reduction of the ADM equations is weakly hyperbolic and in [94] that the standard finite differencing applied to weakly hyperbolic systems results in ill-posed systems.

As a result of the continued problems encountered in evolutions using the ADM equations, a wealth of alternative formulations of the Einstein equations has been suggested in the literature [66, 267, 139, 18, 51, 188, 65, 144, 260, 228]. To date, however, only two of these have been demonstrated to facilitate long-term stable evolutions of black-hole binary spacetimes. These are the Baumgarte-Shapiro-Shibata-Nakamura (BSSN) system [267, 51] and the generalized harmonic gauge (GHG) formulation [144, 247]. We will now discuss these two systems in some more detail.

3.1.1 The BSSN system

The BSSN system results from the ADM equations by applying the following modifications. First, the extrinsic curvature is split into its trace and a tracefree part. Second, a conformal transformation is applied to the three-metric and the extrinsic curvature. Finally, a contracted version of the Christoffel symbols of the conformal metric is introduced as an additional variable. The BSSN variables are then given by

$$\begin{aligned} \phi &= \frac{1}{12}\ln(\det\gamma_{ij}), & \tilde{\gamma}_{ij} &= e^{-4\phi}\gamma_{ij}, \\ K &= \gamma_{mn}K^{mn}, & \tilde{A}_{ij} &= e^{-4\phi}\left(K_{ij}-\frac{1}{3}\gamma_{ij}K\right), \\ \tilde{\Gamma}^i &= \tilde{\gamma}^{mn}\Gamma^i_{mn} = -\partial_m\tilde{\gamma}^{im} \end{aligned} \tag{3.1}$$

This corresponds to a rearrangement of the degrees of freedom which is similar to the York-Lichnerowicz split underlying most of the initial data calculation which we will discuss below in Sec. 3.3. Expressing the ADM equations in terms of these variables leads to the BSSN system

$$
\begin{aligned}
\partial_t \tilde{\gamma}_{ij} &= \beta^m \partial_m \tilde{\gamma}_{ij} + 2\tilde{\gamma}_{m(i}\partial_{j)}\beta^m - \frac{2}{3}\tilde{\gamma}_{ij}\partial_m\beta^m - 2\alpha\tilde{A}_{ij}, && (3.2)\\
\partial_t \phi &= \beta^m\partial_m\phi + \frac{1}{6}(\partial_m\beta^m - \alpha K), && (3.3)\\
\partial_t \tilde{A}_{ij} &= \beta^m\partial_m\tilde{A}_{ij} + 2\tilde{A}_{m(i}\partial_{j)}\beta^m - \frac{2}{3}\tilde{A}_{ij}\partial_m\beta^m + e^{-4\phi}\left(\alpha\mathcal{R}_{ij} - D_iD_j\alpha\right)^{\mathrm{TF}}\\
&\quad +\alpha\left(K\,\tilde{A}_{ij} - 2\tilde{A}_i{}^m\tilde{A}_{mj}\right), && (3.4)\\
\partial_t K &= \beta^m\partial_m K - D^mD_m\alpha + \alpha\left(\tilde{A}^{mn}\tilde{A}_{mn} + \frac{1}{3}K^2\right), && (3.5)\\
\partial_t\tilde{\Gamma}^i &= \beta^m\partial_m\tilde{\Gamma}^i - \tilde{\Gamma}^m\partial_m\beta^i + \frac{2}{3}\tilde{\Gamma}^i\partial_m\beta^m + 2\alpha\tilde{\Gamma}^i_{mn}\tilde{A}^{mn} + \frac{1}{3}\tilde{\gamma}^{im}\partial_m\partial_n\beta^n + \tilde{\gamma}^{mn}\partial_m\partial_n\beta^i\\
&\quad -\frac{4}{3}\alpha\tilde{\gamma}^{im}\partial_m K + 2\tilde{A}^{im}\left(6\alpha\partial_m\phi - \partial_m\alpha\right) - \left(\sigma + \frac{2}{3}\right)\left(\tilde{\Gamma}^i - \tilde{\gamma}^{mn}\tilde{\Gamma}^i_{mn}\right)\partial_k\beta^k, && (3.6)
\end{aligned}
$$

where the superscript $^{\mathrm{TF}}$ means that we take the trace free part of the preceding expression. The last term on the right hand side of Eq. (3.6) vanishes in the continuum limit by virtue of the definition of $\tilde{\Gamma}^i$ in Eq. (3.1). It has been shown in [298], however, to cure instability problems observed in simulations which do not employ octant symmetry [15]. In practice, setting the free parameter $\sigma = 0$ proves satisfactory. Alternatively to using this term, Alcubierre *et al.* [17] achieve stable evolutions by recalculating $\tilde{\Gamma}^i$ from the metric $\tilde{\gamma}_{ij}$ whenever it appears on the right hand side of Eqs.(3.2)-(3.6) in undifferentiated form. So far, all successful implementations of the BSSN equations also require us to enforce the vanishing of the trace of $\tilde{A}_{ij}$. This is realized numerically by replacing $\tilde{A}_{ij}$ with $\tilde{A}_{ij} - \tilde{\gamma}_{ij}\tilde{\gamma}^{mn}\tilde{A}_{mn}$ after each time step. Some codes also enforce in a similar way the constraint $\det\tilde{\gamma}_{ij} = 1$.

A further modification of the BSSN system has been introduced by Campanelli *et al.* [98] who evolve the conformal factor in terms of the variable $\chi = e^{-4\phi}$. Using this "χ-version" of the BSSN system has in some instances been found to result in better convergence properties [86]. Similarly, Marronetti *et al.* [215] report beneficial behavior when evolving $W \equiv e^{-2\phi}$ instead.

The hyperbolicity of the BSSN system was studied in [259] and provided first insight into how well-posedness of the BSSN system is actually achieved. The sensitivity of the hyperbolicity properties of the system under minor changes in the equations may also explain why certain modifications, such as the enforcement of $\mathrm{tr}\tilde{A}_{ij} = 0$, appear to be necessary to obtain long-term stability. Notwithstanding the various open questions underlying the stability properties of the different formulations of the Einstein equations, the BSSN system has become the most popular choice in practice for writing the Einstein equations in simulations of black hole and/or neutron star binaries.

3.1.2 The generalized harmonic formulation

In contrast to the BSSN system, the generalized harmonic formulation is not derived from the ADM equations. Instead, it is based on the four-dimensional version of the Einstein equations in harmonic gauge. The harmonic gauge condition is

$$\Box x^{\alpha} \equiv \nabla^{\mu}\nabla_{\mu}x^{\alpha} = 0, \tag{3.7}$$

and casts the Einstein equations in a particularly convenient form. Specifically, the Ricci tensor can be written as

$$R_{\alpha\beta} = -\frac{1}{2}g^{\mu\nu}\partial_{\mu}\partial_{\nu}g_{\alpha\beta} + \ldots, \tag{3.8}$$

where the dots denote further terms containing the metric and its first derivatives, but no second derivatives. The principal part of the Einstein equations $R_{\alpha\beta} = 0$ is therefore identical to that of the wave equation which has made this gauge very popular in analytic studies of the Einstein equations (see e. g. [88]).

Even though this structure is also very appealing from a numerical point of view, it has not been used successfully in black hole simulations. It has been shown by Garfinkle [144] how one can generalize this system to accommodate arbitrary gauge choices while still preserving the wave-like character of the principal part. This is realized by introducing the source functions

$$H_{\alpha} = \Box x_{\alpha}, \tag{3.9}$$

as first introduced by Friedrich [138]. In the special choice of harmonic gauge $H_{\alpha} = 0$. With these functions, the Einstein equations in vacuum can be written as

$$R_{\alpha\beta} = -\frac{1}{2}g^{\mu\nu}\partial_{\mu}\partial_{\nu}g_{\alpha\beta} + \ldots - \frac{1}{2}\left(\partial_{\alpha}H_{\beta} + \partial_{\beta}H_{\alpha}\right), \tag{3.10}$$

where again the dots denote terms only involving the metric and its first derivative. The introduction of the auxiliary gauge functions H_{α} thus preserves the wave-like principal part of the Einstein equations for arbitrary gauge choices.

As yet, no simple geometric interpretation of the H_{α} analogous to that of lapse

α and shift β^i has been found, but the two sets of gauge functions are connected via the differential relations [248]

$$H_\mu n^\mu = -K - \frac{1}{\alpha^2}\left(\partial_t \alpha - \beta^i \partial_i \alpha\right), \tag{3.11}$$

$$\perp^i{}_\mu H^\mu = \frac{1}{\alpha}\gamma^{ik}\partial_k \alpha + \frac{1}{\alpha^2}\left(\partial_t \beta^i - \beta^k \partial_k \beta^i\right) - \gamma^{mn}\Gamma^i_{mn}. \tag{3.12}$$

Just as lapse and shift need to be specified in addition to the evolution of the BSSN equations, the functions H_α need to be specified by the user in the GHG system. The definition (3.9) of H_α takes on the role of a constraint

$$C_\alpha = H_\alpha - \Gamma^\mu_{\mu\alpha} + g^{\mu\nu}\partial_\mu g_{\nu\alpha}, \tag{3.13}$$

which can be shown to be related to the Hamiltonian and momentum constraints via [203]

$$[\mathcal{H},\ \mathcal{M}_i] = (G_{\alpha\beta} - 8\pi T_{\alpha\beta})n^\beta = \nabla_{(\alpha}C_{\beta)}n^\beta - \frac{1}{2}n_\alpha \nabla_\beta C^\beta. \tag{3.14}$$

While these constraints are propagated in the continuum limit by the evolution equations, this can become problematic in numerical simulations, where constraints will always be violated due to numerical inaccuracies. If these constraint violations grow without control, they may give rise to numerical instabilities.

We have already seen, how the addition of the constraint to the right hand sides of the evolution equations can cure numerical instabilities in the case of the BSSN equation (3.6) for the variable $\tilde{\Gamma}^i$. A similar cure using the constraint C_α as suggested by Gundlach *et al.* [154] turned out to be an important ingredient in Pretorius' first simulation of a black-hole binary through inspiral and merger [247]. These cases represent good examples of the intricacies involved in numerically evolving the Einstein equations.

For further details of the generalized harmonic formulation the reader is referred to Sec. III C of [252].

3.2 Gauge conditions

We have seen in the previous sections that the Einstein equations do not predict the evolution of the gauge variables α and β^i in the BSSN system or H_α in the generalized harmonic formulation. Instead, these functions are specified by the user and represent the coordinate freedom of general relativity. Indeed, any choice for these functions is guaranteed not to affect the physical properties of the system under investigation. If the choice of gauge has no impact on the physics of the system, one may wonder why it it necessary to discuss gauge conditions at all. The reason is that the choice of gauge does have a strong impact on the performance and stability of a numerical code. A simple example to illustrate this problem arises in evolutions of a single Schwarzschild black hole [274]: A simulation starting on a time-symmetric hypersurface using geodesic slicing, i.e. $\alpha = 1$ everywhere, in combination with vanishing shift, will hit the singularity after the short coordinate time of $\Delta t = \pi M$, where M is the mass of the Schwarzschild hole. Because of the divergent nature of the metric components at the singularity, a computer is not capable of representing the singularity using numbers and instead produces "non-assigned-numbers" (nan) at some grid-points. These quickly swamp the computational grid and render the entire simulation useless.

A common strategy to avoid this problem is to reduce the lapse function α as the hypersurfaces get closer to a singularity [201, 274, 17]. The corresponding slow down in the advance of proper time "bends" the hypersurfaces around the singularity. Such singularity avoiding slicings are frequently used in numerical codes. A potential danger arising out of this procedure, however, is the so-called slice stretching (see for example Sec. V B in [23]). Whereas the advance of proper time at points x^i close to the black hole singularity is slowed down, points further away from the black hole advance almost normally, i.e. with $\alpha \approx 1$. As the evolution proceeds, these differences accumulate and eventually neighboring points on the numerical grid represent spacetime events far away from each other. Unless the shift vector is carefully chosen to counteract this effect, this leads to resolution problems near the black hole and gives rise to numerical instabilities.

Alternatively to specifying the slicing in terms of the lapse α, it turns out to be beneficial in certain situations to use a densitized version $Q \equiv \gamma^{-n/2}\alpha$, where γ is the determinant of the physical three-metric and n a free parameter. Most notably, Khokhlov *et al.* [185] have shown that the use of fixed gauge conditions, that is specification of the gauge in terms of prescribed functions of the spacetime coordinates for α and β^i almost always yields an ill-posed system. Using fixed gauge in combination with a densitized lapse with $n > 0$, however, has been shown to result in well-posedness. This approach has been successfully used in head-on collisions of Kerr-Schild data [281, 280]. The use of a densitized lapse has also played an important role in hyperbolicity studies of the Einstein equations (see, for example, [142, 188, 94, 259]), and has been used as an ingredient in alternative formulations of the Einstein equations (see, for example, [195]). In the case of gauge conditions formulated in terms of differential equations, as for example in the moving puncture approach discussed below, numerical experiments indicate, that the original lapse function performs equally satisfactorily as its densitized counterpart and is the preferred choice for simplicity reasons.

The detailed study of the impact of gauge conditions and the reasons why some conditions work so much better than others is still subject to ongoing research and there remain many questions, in particular in connection with the shift vector. To date, the choice of gauge conditions in numerical codes has been motivated by the avoidance of singularities and slice stretching, but failsafe recipes for their derivation are currently not known. Instead, the selection of gauge conditions is based on a combination of educated guessing and empirical testing in black hole simulations.

Gauge conditions used in early numerical simulations were inspired by geometrical ideas. The maximal slicing condition $K = 0$ derives its name from the fact that the three-dimensional volume of spatial hypersurfaces obeying this condition are maximal [274]. This condition leads to an elliptic equation for the lapse function and is therefore computationally expensive and non-trivial to implement. Similarly, the minimization of the strain (cf. Eq. (4.5) of [274]) leads to an elliptic condition for the shift vector. To the authors knowledge, these gauge conditions have not yet been implemented in more recent simulations of black hole mergers, so that it remains unclear, to what extent the instabilities encountered in early simulations are based on this choice of gauge. In any case, maximal slicing and the minimal distortion shift form the basis of many modified gauge conditions employed in the course of the following decades.

A remarkable simplification of the implementation of gauge conditions like maximal slicing is the idea of driver conditions [46, 15, 17]. Here, the elliptic equation is replaced by a parabolic or hyperbolic equation which drives the gauge ever closer to an equilibrium state similar to the equation of heat conduction. The key numerical advantage is that such evolution equations are substantially easier to implement because there arises no need for solving elliptic equations.

The idea of driver conditions was particularly appealing for stationary or quasi-stationary spacetimes and has commonly been used for puncture type initial data (see Sec. 3.3 below). By using co-moving or co-rotating coordinates, most of the black hole dynamics can be absorbed in the coordinates and the spacetime variables show little actual change in coordinate time [17, 87, 16, 307, 123]. The most prominent conditions are the "1+log" slicing

$$\partial_t \alpha = -2\alpha K, \tag{3.15}$$

and a second order in time Γ-driver condition for the shift. Different groups use slightly different Γ-driver conditions. For example, the version reported in [16] is

$$
\begin{aligned}
\partial_t \beta^i &= \frac{3}{4}\alpha^p \psi_{\mathrm{BL}}^{-n} B^i, && (3.16)\\
\partial_t B^i &= \partial_t \tilde{\Gamma}^i - \eta \beta^i, && (3.17)
\end{aligned}
$$

with parameter choices $p = 1$ or 2, $n = 2$ or 4 and $\eta \in [2, 5]$. In these simulations, the conformal factor is split into an analytic part ψ_{BL} of the Brill-Lindquist solution and a regular remainder (see, for example, Sec. IV C of Ref. [17]).

Gauge conditions were studied in a more general way by Bona and Massó [67] (for further discussion see also [14] and references therein). The above mentioned harmonic gauge as well as the driver conditions are special cases of the Bona-Massó family of gauge conditions [67]. This general class of gauge conditions has been used in various analytic studies to investigate singularity avoidance and the formation of gauge shocks [12, 253, 13].

While these ingredients still form a major part of the current generation of numerical codes, the simulation of black-hole binaries through merger has so far only been successfully accomplished after abandoning the idea of co-rotating coordinates and instead allowing the black holes to move throughout the computational domain. The first inspiral and merger was obtained by Pretorius [247] who used the generalization of the harmonic formulation described in the previous section. Specifically, he constructed his gauge by evolving the gauge functions according to.

$$
\begin{aligned}
\Box H_t &= -\xi_1 \frac{\alpha - 1}{\alpha^\eta} + \xi_2 n^\nu \partial_\nu H_t, && (3.18)\\
H_i &= 0. && (3.19)
\end{aligned}
$$

A few months after Pretorius' breakthrough, the relativity groups of the University of Brownsville and NASA Goddard independently discovered an evolution method now commonly referred to as the moving-puncture approach [98, 41]. In contrast to previous puncture simulations, the conformal factor is no longer decomposed into an analytically known part plus a regular piece but is instead evolved as a single quantity. In combination with modifications of the "1+log" slicing and the Γ-driver condition which allow the black holes to move across the computational domain they obtain a remarkably straightforward technique for evolving black-hole binaries. Several groups have now developed codes using this moving puncture method. All codes use the modified "1+log" slicing condition

$$\partial_t \alpha = \beta^i \partial_i \alpha - 2\alpha K, \tag{3.20}$$

but they differ in the modifications applied to the $\tilde{\Gamma}$-driver condition for the shift vector. A sample of the exact gauge conditions reported by various groups is given as follows

Code	Reference		
UTB	[98]	$\partial_t \beta^i = B^i,$	$\partial_t B^i = \frac{3}{4}\partial_t \tilde{\Gamma}^i - \eta B^i,$
Goddard	[41]	$\partial_t \beta^i = \frac{3}{4}\alpha B^i,$	$\partial_t B^i = \partial_0 \tilde{\Gamma}^i - \eta B^i,$
PSU	[169]	$\partial_t \beta^i = \frac{3}{4}\alpha B^i,$	$\partial_t B^i = \partial_0 \tilde{\Gamma}^i - \eta B^i,$
Lean	[278]	$\partial_t \beta^i = B^i,$	$\partial_t B^i = \partial_t \tilde{\Gamma}^i - \eta B^i,$
Bam	[86]	$\partial_0 \beta^i = \frac{3}{4} B^i,$	$\partial_0 B^i = \partial_0 \tilde{\Gamma}^i - \eta B^i,$
AEI	[41]	$\partial_t \beta^i = \frac{3}{4}\alpha B^i,$	$\partial_t B^i = \partial_0 \tilde{\Gamma}^i - \eta B^i,$

where $\partial_0 = \partial_t - \beta^i \partial_i$. The free parameter η has an influence on the eventual coordinate radius of the black holes [86] and typical choices for this parameter are in the range $0.5 \le \eta \le 2$ with no significant impact on the quality of the simulations except for instabilities arising at outer refinement boundaries observed in some cases for large values of η (cf. Ref. [279]). A more detailed analysis of different gauge conditions in moving puncture evolutions of black-hole binary spacetimes is given in van Meter *et al.* [221].

3.3 Initial data

We have so far discussed the differential equations determining the time evolution of the spacetime hypersurfaces. In order to start an evolution, however, we first need to construct an initial data set. This task confronts us with two problems. First, the initial data need to satisfy the Hamiltonian and momentum constraints (2.20), (2.21). The second problem is that the initial data set must represent a snapshot of an astrophysically realistic system. The construction of initial data is an entire branch of research in numerical relativity and we cannot cover all aspects of this work in this report. For a more comprehensive summary of the initial data calculation we refer the reader to Cook's review article [110].

Most of the work on solving the constraints is based on the York-Lichnerowicz split [201, 299, 300, 301, 302], which rearranges the degrees of freedom via a conformal rescaling and the split of the extrinsic curvature into its trace and a tracefree part according to

$$\gamma_{ij} = \psi^4 \tilde{\gamma}_{ij}, \tag{3.21}$$

$$K_{ij} = A_{ij} + \frac{1}{3}\gamma_{ij} K. \tag{3.22}$$

It turns out to be convenient to further decompose the tracefree part of the extrinsic curvature into a longitudinal and a transverse part. Two approaches to this decomposition have been used. In the physical traceless decomposition [233, 234, 235], this procedure is applied directly to the traceless part of the extrinsic curvature A_{ij}; in the conformal traceless decomposition [302, 305], it is applied to a conformally rescaled version

$$A_{ij} = \psi^{-10} \tilde{A}_{ij} \qquad \text{or} \qquad A_{ij} = \psi^{-2} \tilde{A}_{ij}. \tag{3.23}$$

Both approaches eventually require us to specify the conformal metric $\tilde{\gamma}_{ij}$, the trace of the extrinsic curvature K and the symmetric transverse tracefree part of the extrinsic curvature. The four constraint equations are solved with these freely specified functions and provide solutions for the conformal factor ψ and the potential of the longitudinal part of the extrinsic curvature. The detailed equations can be found in Sec. 2.2 of [110]. A particularly useful property of these splits is that the momentum constraint decouples from the Hamiltonian constraint if we assume conformal flatness, i. e. $\tilde{\gamma}_{ij} = \delta_{ij}$, and K is a constant. This simplification is frequently used in the practical calculation of initial data sets.

More recently, an alternative approach, called the thin-sandwich decomposition [304], has become a very popular alternative to this approach. Loosely speaking, the key idea here is to replace the extrinsic curvature in terms of the time derivative of the metric using the evolution equation (2.15) for the metric. Eventually, one freely specifies the conformal metric $\tilde{\gamma}_{ij}$, its time derivative, the trace of the extrinsic curvature and a conformally rescaled version of the lapse function. Solving the constraint not only provides us with the extrinsic curvature and the three-metric on the initial slice, but also with a lapse function and shift vector. The advantage of this approach is that we can directly impose a condition on the time derivative of the three-metric and obtain lapse and shift corresponding to this condition. This is particularly useful in the construction of quasi-equilibrium data, as for example a circularized binary in co-rotating coordinates, where the time derivative of the metric is assumed to vanish. A more detailed description of the thin-sandwich approach is presented in Sec. 2.3 of [110].

Having obtained the framework which facilitates an efficient solving of the constraint equations, there remains the second difficulty we mentioned at the beginning of this section. How do we obtain realistic black-hole initial data? There are two main approaches to this problem. First we discuss the generalization of analytically known single black hole solutions.

As one might expect, the approaches discussed above provide relatively simple methods to derive the Schwarzschild solution. If, for example, we assume conformal flatness and a time symmetric initial data set, i.e. $K_{ij} = 0$, the momentum constraints can be shown to be trivially satisfied and the Hamiltonian constraint becomes

$$\bar{\nabla}^2 \psi = 0, \tag{3.24}$$

where $\bar{\nabla}$ is the flat space Laplace operator. The simplest solution to this equation is

$$\psi = 1 + \frac{M}{2r}, \tag{3.25}$$

which gives us the Schwarzschild solution in isotropic coordinates. This solution can be generalized straightforwardly to any number of black holes. Indeed, the linearity of the Hamiltonian constraint (3.24) immediately allows us to superpose solutions to obtain [224, 81]

$$\psi = \sum_{i=1}^{N} \frac{M_i}{|\vec{r} - \vec{r}_i|} \tag{3.26}$$

These are known as Brill-Lindquist initial data and represent N holes at positions $\vec{r}_i$. It can be shown that each of the poles in these solutions corresponds to spatial infinity in an asymptotically flat hypersurface, that is, each hole provides a connection to a different universe, so that we have in total $N + 1$ universes. A similar solution where all holes provide a connection between the same two asymptotically flat universes has been found by Misner [225].

Both, the Brill-Lindquist and the Misner data, represent N black holes at the moment of time symmetry, that is, black holes with vanishing linear and angular momentum. It is a remarkable property that analytic solutions for the momentum constraints can even be found in the generalized case of Misner data with non-vanishing momenta [74]. These data are commonly referred to as Bowen-York data and start again with the simplifying assumption of conformal and asymptotic flatness as well as maximal slicing $K = 0$. With the analytic solution of the momentum constraints, there merely remains the task of solving numerically the Hamiltonian constraint for the conformal factor. Even more remarkable, the total linear momenta $\vec{P}_i$ and spins $\vec{S}_i$ associated with the individual holes in the limit of isolated holes appear as explicit parameters in the analytic Bowen-York extrinsic curvature and thus provide us with a straightforward physical interpretation of the initial data. The total energy of the spacetime is also obtained relatively straightforwardly from the $1/r$ falloff term of the conformal factor as $r \to \infty$. The corresponding generalization to Brill-Lindquist data was developed by Brandt and Brügmann [79]. These data are known as puncture data and form the starting point for most of the so-called "moving puncture simulations" mentioned above.

In spite of the great popularity of these initial data, there are some concerns associated with the underlying simplifying assumptions. First, it has been shown that there are no spatial hypersurfaces of the Kerr spacetime with non-zero spin parameter for which the three-metric can be written in a conformally flat way [143]. It turns out that the initial data thus calculated represent the snapshot of a rotating black hole plus a non-vanishing gravitational wave content. We will return to this spurious gravitational radiation further below. At this point, we merely note that all binary-black hole data successfully evolved to date contain such spurious initial radiation. In comparison with the merger waveform, however, this spurious or junk radiation is rather low in amplitude and appears to represent a smaller problem than anticipated, at least in the case of non or slowly rotating black holes with small linear momentum. Alternative non-conformally flat black hole initial data based on generalizations of the single hole Kerr-Schild solution [183, 184] have been investigated in initial data studies as well as numerical evolutions [216, 80, 214, 213, 70, 280, 278].

A popular alternative to puncture type initial data is often referred to as "excision data". The idea here is to incorporate black holes in the form of horizon boundary conditions into the initial data. A black hole is defined by the presence of an event horizon, that is, a boundary which defines a region of spacetime from which null-geodesics cannot extend all the way to null-infinity. A more convenient framework encapsulating horizons in numerical relativity is that of apparent and isolated horizons ([124, 33, 73, 150] and references therein) which provides boundary conditions for the metric and extrinsic curvature components at the horizon. These conditions are particularly convenient to apply in combination with the quasi-equilibrium assumption and, thus, the thin-sandwich approach. Black hole data have been constructed along these lines in [111, 112, 242, 181, 114, 28] and form the starting point for most of the simulations performed with the generalized harmonic formulation [39, 90, 243, 78].

We conclude this discussion with a counting of the physical parameters of a general black-hole binary initial data set. First, we need to fix the total scale of our problem which corresponds to fixing the total ADM mass of the system. Once we have fixed the scale, six parameters are required to determine the spins $\vec{S}_1$ and $\vec{S}_2$ of the two holes and one parameter for the mass ratio $q = M_1/M_2$. In general we also need to take into account the eccentricity of the orbits. The emission of gravitational waves has the effect of circularizing the orbit [241], however, so that for many purposes, it is sufficient to consider quasi-circular orbits[1]. In Most cases, we therefore have seven physical parameters (see, however, [279, 172] and references therein for investigations of eccentric binaries and their relevance in astrophysics). In practice, current numerical codes are able to evolve a binary for at most a few tens of orbits at acceptable computational cost, so that we need to specify an initial separation of the binary. This can be done, for example, in the form of a coordinate separation or an initial orbital frequency. Constructing a quasi-circular orbit then requires the accurate specification of the orbital angular momentum corresponding to a circular orbit. Three methods have been used in the literature to minimize the eccentricity of the initial configuration. The effective potential method [109, 48] is inspired by Newtonian physics and starts with a fixed value of the orbital angular momentum. It then varies the separation of the orbit and defines the quasi-circular configuration as that which minimizes the binding energy of the binary. The second method is based on the approximate stationarity of a circular binary in co-rotating coordinates. Mathematically, this corresponds to the existence of an approximate helical Killing vector which is used to impose the approximate symmetry of the binary under rotations [149, 151, 290] (see also [289] for a sequence of parameters for quasi-circular puncture initial data sets). Finally, the post-Newtonian formalism predicts the angular momentum of a binary with given separation on a quasi-circular orbit (see, formula (64) in [86] based on the 3PN accurate calculations in ADM-transverse-traceless gauge of [118]).

A comparison of the three methods applied to a non-spinning, equal-mass binary starting about two orbits prior to merger is given in [86], and finds excellent agreement between the resulting momentum parameters. The phase of the resulting waveforms turns out to be rather sensitive to the initial parameters, however, so that the three methods lead to notably different merger times. We will return to the issue of residual eccentricity in the initial data below in Sec. 6.1 when we discuss methods to further improve the initial momentum parameters.

[1]The term 'quasi' refers to the fact that the orbit is continuously shrinking because of the energy loss of the system

3.4 Mesh refinement and outer boundary conditions

We now turn our attention to the more technical aspects of numerical simulations of black-hole spacetimes. The majority of codes solve the set of partial differential equations determining the evolution of the binary using standard finite differencing techniques (see, for example, Sec. 2.3 of [277] and Sec. II of [307]). The only exception is the Caltech-Cornell effort [262] which employs spectral methods (see, for example, [152]). For both methods, the accuracy of the numerical simulations is determined by the resolution, that is the total number of grid points. Because of the three-dimensional nature of the grids, a mild increase in resolution results in a substantial increase in computational costs and memory requirements.

A major difficulty in performing such simulations arises out of the presence of different length scales in the spacetimes under consideration. The black hole size is approximately given by the mass of the hole M. Gravitational waves, however, have wavelengths about one or two orders of magnitude larger and need to be extracted sufficiently far away from the strong-field region, ideally in the wave-zone. This wave-zone starts approximately at distances of $10^2\ M$. In order to avoid contaminations from the outer boundary, the computational domain needs to be several times as large as that value. With current computational resources, it is impossible to evolve such large domains with the resolution required to resolve the steep gradients near the black hole horizons. The only solution to this problem is the use of mesh-refinement, that is, the use of different resolutions in different parts of the computational domain. This applies both, to the finite differencing codes as well as the Caltech-Cornell spectral code.

Mesh refinement has been made popular in numerical relativity by Choptuik who thus obtained the required accuracy in his discovery of critical phenomena [107]. Because of the movement of black holes, it is not sufficient to use fixed mesh refinement, where the regions of increased resolutions remain stationary in time. Mesh refinement where the zones of refinement change in time is called adapted and generally measures the steepness of the gradients to determine what resolution is needed in a particular region of the domain. The implementation of mesh-refinement in black-hole evolutions does not require the full machinery of adapted mesh-refinement because it is relatively straightforward to locate black holes via their apparent horizons and black holes are rigid objects and preserve their shape to a remarkable degree. A common approach in the current generation of black-hole codes is the so-called moving boxes method. That is, the computational grid

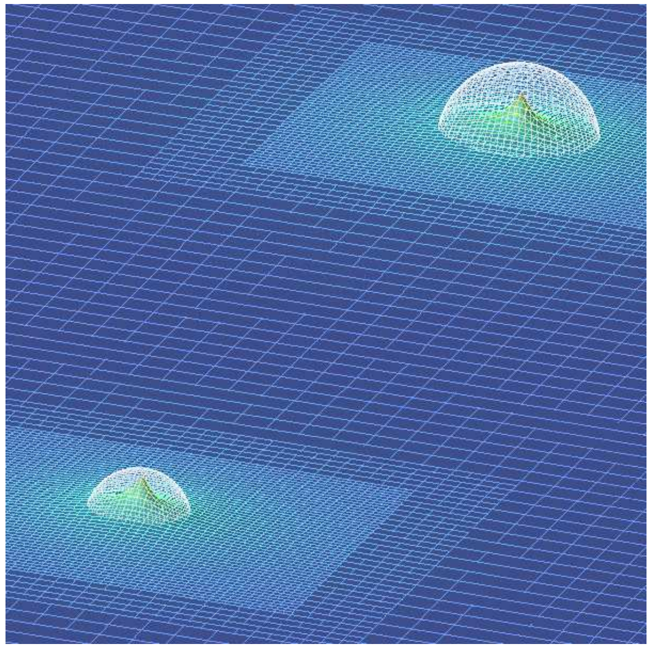

Figure 3.1: Illustration of mesh-refinement in black hole simulations.

consists of a nested set of rectangular boxes with decreasing size and increasing resolution. A subset of these boxes follows the black hole motion and thus guarantees that sufficient resolution is maintained near the black holes. This is illustrated in Fig. 3.1 where the black holes are represented by their apparent horizons (white hemispheres).

While mesh-refinement is conceptually rather straightforward, it represents a formidable book keeping exercise in general relativistic simulations and also a potential source of instabilities. Indeed, it is often hard to generalize stability studies to numerical techniques with mesh-refinement and commonly the success of a method is only established in practice by evolving black-hole data.

An alternative to mesh-refinement is the use of coordinates which are "stretched" further away from the black holes and thus result in an effectively lower resolution. These so-called "fish-eye" coordinates allow one to push the outer boundary to larger radii at acceptable computational costs [35].

Fixed mesh-refinement was first used in black-hole simulations by Brügmann [83] in fixed form for a dynamically sliced Schwarzschild hole. Pretorius' first simulations of a black-hole inspiral and merger used mesh-refinement based on a modified Berger-Oliger [56] scheme (see [250, 249] for details). Further refinement packages include Carpet [263, 1] which provides mesh-refinement for several codes [169, 278, 103, 192] using the Cactus computational toolkit [2], Paramesh [208] used by the Goddard group [40], Samrai [3] which is used by openGR [4] and had [5, 202] used for mixed binary evolutions in [19].

A closely related topic concerns the specification of conditions at the outer boundaries. A potential danger arising from outer boundary conditions is the violation of the constraints. Furthermore, it is not immediately clear, to what extent a given set of boundary conditions preserves the hyperbolicity of the set of evolution equations. Several conditions ensuring the constraints and/or the hyperbolicity have been suggested in the literature [140, 95, 141, 261, 156, 187, 203]. To our knowledge, however, only that of [203] has been successfully used for black-hole-binary evolutions in the Caltech-Cornell code [243, 78]. Pretorius [247, 249] instead uses a compactification of the spacetime. In contrast to characteristic formulations where compactification is natural and common, it inevitably implies a loss of resolution at sufficiently large distances from the binary when applied to slices approaching spatial infinity. The reason is simply that the characteristics, i.e. null geodesics are curves of constant phase of gravitational waves whereas space-like curves are not. Pretorius solves this difficulty by using numerical dissipation in the outer parts of the computational domain and thus avoids high-frequency noise.

All other codes use the relatively simple outgoing Sommerfeld condition; see, for example, Sec. VI A of Alcubierre *et al.* [17]. For the studies performed so far, this choice appears to provide sufficient accuracy provided the outer boundary is located at sufficiently large distances from the strong field sources. It remains to be seen, to what extent improvements will be needed in future studies.

3.5 Singularity treatment

A further complication in black hole simulations normally not encountered in other areas of computational physics is the presence of singular points in the spacetimes. Two types of singularities can arise in general relativity; coordinate singularities, as for example the famous $r = 2M$ in the Schwarzschild metric, and physical singularities. If the code encounters either of these, it will crash because metric components will diverge at the singularities. We have already discussed this point in the context of singularity avoiding slicings which slows down the evolution in the vicinity of singular points.

An alternative to this approach has been suggested by Unruh as cited in [285] and is based on the cosmic censorship conjecture which stipulates that there exist no naked singularities. Instead, a singularity will always be surrounded by a horizon, that is, a causal boundary that disconnects a region of spacetime from the exterior in the sense that no information, not even light, can travel from the inner region to the exterior. In consequence, the external spacetime is completely independent from what is happening in the interior. It is possible therefore, to remove this interior part containing the singularity from the computational domain and evolve exclusively the exterior spacetime. This is graphically illustrated in Fig. 3.2, where

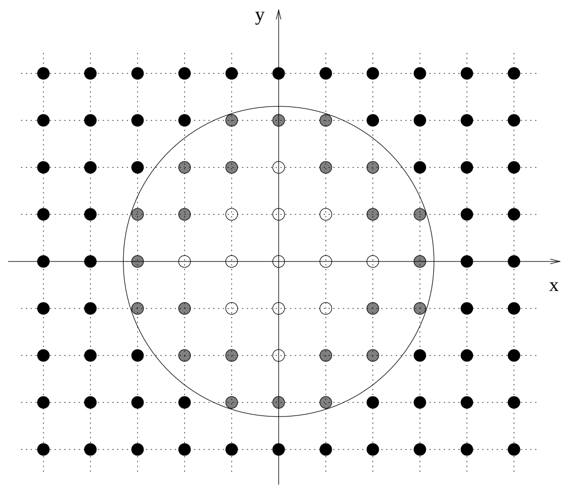

Figure 3.2: Illustration of black hole excision.

the dots represent grid points and the circle the horizon. Points outside the horizon are evolved normally (black dots). Inside the horizon there is a layer of boundary points (grey) where data is commonly obtained from extrapolation from exterior points. The inner points (white) are simply ignored, that is "excised" from the numerical simulation.

Black hole excision has been used in the 1990s using a technique called causal differencing [266, 24]. More recent implementations in finite differencing codes have been based on straightforward extrapolation. The so-called "simple excision" method of Alcubierre and Brügmann [15] provided a remarkably straightforward method to obtain long-term stable evolutions of single black holes and has also been used in simulations of orbiting binaries in co-rotating coordinates [87, 123]. More general techniques accommodating moving black holes via dynamic excision have been used in [80, 270, 248, 280, 247, 243]

An alternative method to handle the coordinate singularity inherent to puncture data was the decomposition of the conformal factor. In the simulation, only the regular piece was evolved. The recent "moving puncture" simulations differ from that approach in that they evolve the entire conformal factor. One consequence is that the nature of the coordinate singularity also changes its nature [165, 161, 50, 82, 287, 162] and may loose contact with the asymptotic spatial infinity. Given the finite numerical resolution, however, these features inside the black hole horizon are not resolved in a numerical simulation and the moving-puncture method appears to provide a kind of automatic and natural excision.

Among the current generation of black hole codes, explicit excision is implemented in the generalized harmonic codes of Pretorius and the Caltech-Cornell effort and in the second order accurate version of Sperhake's Lean code. The implementation in the spectral Caltech-Cornell code is special in the sense that they use a so-called dual-coordinate frame to accommodate the motion of the holes. Using two coordinate systems and transforming variables between these systems avoids the necessity to move the excision region across the computational domain; see [262] for details.

Chapter 4

Diagnostics

Once we have successfully evolved a spacetime containing black holes, there still remains the task of extracting physical information from the simulation. This procedure faces two major difficulties. First, a computer simulation only produces a large set of numbers which represent coordinate dependent quantities. We need to construct physical, that is gauge invariant, combinations from these quantities. A second problem is that not all physical concepts familiar from Newtonian physics are well-defined in general relativity. In particular, this applies to local quantities as for example the energy contained in a particular region of spacetime. In the following we will discuss all important quantities currently used in numerical relativity to extract physical information from the simulations. For this purpose we assume that all ADM variables are known in some part of the spacetime. These variables are the lapse α, the shift β, the three-metric γ_{ij} and the extrinsic curvature K_{ij}. These variables can always be computed straightforwardly from the evolution variables, even if we use a formulation not based on the ADM equations.

4.1 Global quantities

Global quantities provide us with information characterizing the entire spacetime. They are usually defined by evaluating variables at spatial or null infinity. In most contemporary numerical evolutions, the computational domain does not extend all the way to infinity, so that we need to approximate global quantities by calculating them at large but finite distances from the strong field region near the black holes.

The total mass or energy of the spacetime is given by the so-called ADM mass

[30] which is obtained from the three-metric by the surface integral

$$M_{\mathrm{ADM}} = \frac{1}{16\pi} \lim_{r\to\infty} \int_{S_r} \sqrt{\gamma}\gamma^{ij}\gamma^{kl}(\partial_j\gamma_{ik} - \partial_k\gamma_{ij})dS_l, \tag{4.1}$$

Here γ is the determinant of the three-metric, S_r the coordinate sphere $r = \text{const}$, R_m the unit normal field on that sphere and $dS_l = R_l d\theta d\phi$ with standard angular coordinates θ and ϕ.

Similarly, the total linear and angular momentum of the spacetime can be calculated from (see e. g. [302])

$$P_i = \frac{1}{8\pi} \lim_{r\to\infty} \int_{S_r} \sqrt{\gamma}\left(K^m{}_i - K\delta^m{}_i\right) dS_m, \tag{4.2}$$

$$J_i = \frac{1}{8\pi}\epsilon_{il}{}^m \lim_{r\to\infty} \int_{S_r} \sqrt{\gamma}x^l\left(K^n{}_m - K\delta^n{}_m\right) dS_n, \tag{4.3}$$

where $\epsilon_{il}{}^m$ is the three-dimensional Levi-Civita tensor.

We emphasize that all these quantities are by construction time independent. In contrast, the Bondi-mass [69] is evaluated at null infinity, thus takes into account the radiation of energy to null infinity in the form of gravitational waves and varies with retarded time. It is a natural diagnostic tool in characteristic formulations but not directly available in 3+1 evolutions.

4.2 Local quantities

We have already mentioned that it is often impossible to define local concepts of energy and momenta. In the case of black holes, however, it is possible to use the concept of horizons [33] to define mass and spin associated with the horizon and thus with the black hole. Imagine for that purpose a three-dimensional hypersurface Σ and a closed two-dimensional surface S embedded in Σ (see for example Fig. 1 in Ref. [124]. On each point of S one can define in and outgoing null vectors $\hat{n}_\alpha$ and ℓ_α. The expansion of in and outgoing light cones is given in terms of these null vectors by

$$\theta_{(\ell)} = q^{\alpha\beta}\nabla_\alpha \ell_\beta, \qquad \theta_{(\hat{n})} = q^{\alpha\beta}\nabla_\alpha \hat{n}_\beta, \tag{4.4}$$

where $q_{\alpha\beta}$ is the induced two-metric on the surface S. A marginally trapped surface is defined by the condition that the outgoing expansion vanishes $\theta_{(\ell)} = 0$ and the ingoing expansion satisfies $\theta_{(\hat{n})} < 0$. Loosely speaking, this means that all light cones on the trapped surface are tilted inwards to such an extent that light rays cannot escape outwards. In general, a black-hole spacetime has more than one marginally trapped surface and the apparent horizon is defined as the outermost marginally trapped surface.

The main task in a numerical simulation is to locate surfaces S with vanishing expansion $\theta_{(\ell)} = 0$. Various apparent horizon finders have been developed by the numerical relativity community. For more details on the numerical methods to locate the apparent horizon and the physical interpretation of the horizon properties the reader is referred to [49, 22, 124, 178, 33, 286, 194] and references therein.

For the discussion in the remainder of the work, the most important quantity is the irreducible mass of the horizon which is defined in terms of the horizon area by

$$M_{\rm irr} = \sqrt{\frac{A_{\rm AH}}{16\pi}}. \tag{4.5}$$

In the limit of an isolated hole, i.e. a black hole whose interaction with other holes or matter sources is negligible, one can use the world tube of apparent horizons, the so-called isolated horizon, to define the angular momentum associated with the horizon

$$J_{(i)} = \frac{1}{8\pi}\oint_S \phi^m_{(i)} R^n K_{mn} dS, \tag{4.6}$$

where R^n is the outgoing unit normal field on S and $\phi^m_{(i)}$ is the Killing vector associated with the rotational symmetry and the index (i) labels the axis of the rotation, e.g. the x, y or z component of the spin (see [33] for more details). Finally, we can use the spin of the black hole to calculate the total black hole mass M according to Christodoulou's formula [108]

$$M^2 = M_{\rm irr}^2 + \frac{J^2}{4M_{\rm irr}^2}. \tag{4.7}$$

In the limit of a stationary spacetime with a single black hole, this mass corresponds to the ADM mass. In spacetimes with a black-hole binary we can use the individual black hole masses and the ADM mass to define the binding energy

$$E_{\rm b} = M_{\rm ADM} - M_1 - M_2. \tag{4.8}$$

This definition assumes, however, that there are no other forms of energy present in the spacetime. In numerical practice, this condition is normally violated because initial data sets contain some spurious gravitational radiation in addition to the black holes. In many cases, however, this spurious energy content turns out to be small compared with the right hand side of Eq. (4.8) and the resulting error in the binding energy is small.

4.3 Gravitational waves

Arguably the most important information resulting from a simulation of black holes is the amount and structure of the gravitational waves emitted in the course of the inspiral and merger. The gravitational wave signal enables us to calculate the loss of energy and linear and angular momentum of the system and also predicts the strain $h_{+,\times}$ exerted upon a distant gravitational wave detector.

The most common method to extract gravitational waves from a numerical simulation is based on the Newman Penrose formalism [232]. Specifically, one defines a tetrad ℓ^α, $\hat{n}^\alpha$, m^α and $\bar{m}^\alpha$ where $\hat{n}$ and ℓ are ingoing and outgoing null vectors and m is a complex linear combination constructed out of two spatial unit vectors such that

$$-\ell \cdot \hat{n} = 1 = m \cdot \bar{m}, \tag{4.9}$$

and all other inner products vanish.

The Newman-Penrose scalar Ψ_4 is defined in terms of this tetrad and the Weyl tensor as[1]

$$\Psi_4 = C_{\alpha\beta\gamma\delta}\hat{n}^\alpha \bar{m}^\beta \hat{n}^\gamma \bar{m}^\delta. \tag{4.10}$$

In 3+1 simulations, the Weyl tensor is obtained from the fundamental forms according to the Gauss-Codacci equations (2.16)-(2.18). In practice, Ψ_4 is calculated on a sphere of constant coordinate radius $r_{\rm ex}$ and is therefore a function of the angular coordinates θ, ϕ and the time t.

It can be shown that under a tetrad rotation which leaves ℓ and $\hat{n}$ unchanged but rotates m, $\bar{m}$ through an angle ϑ, the Newman-Penrose scalar Ψ_4 transforms into $e^{-2i\vartheta}\Psi_4$, that is as a spin-weight -2 field. It is therefore convenient to decompose Ψ_4 in a series of spin-weight -2 spherical harmonics $Y^{-2}_{\ell m}$, where $\ell = 2, ...$ and $m = -\ell, ..., \ell$ denote the multipole indices [288]. At extraction radius $r_{\rm ex}$ we can describe the gravitational wave signal in the form of mode coefficients $\psi_{\ell m}(t)$ of the series expansion

$$\Psi_4 = \sum_{\ell,m} \psi_{\ell m}(t) Y^{-2}_{\ell m}(\theta,\phi). \tag{4.11}$$

It turns out that the complete signal is often dominated by a small number of modes, normally including the quadrupole moments $\ell = 2$. It is for this reason that gravitational waveforms are often presented in the form of one-dimensional plots showing some $\psi_{\ell m}(t)$.

In order to ensure that Ψ_4 is a measure for the outgoing gravitational waves,

[1] There are ambiguities in the overall sign of this definition in the literature

the tetrad has to be chosen with care. In the case of spacetimes perturbatively close to the Kerr-solution, the appropriate choice is the Kinnersley tetrad [190]. In general numerical simulations, however, it is not clear how one can unambiguously identify the Kinnersley tetrad. Instead, one commonly constructs the tetrad from the timelike unit normal field n and three spatial triad vectors u, v and w according to

$$\ell^\alpha = \frac{1}{\sqrt{2}}\left(n^\alpha + u^\alpha\right), \tag{4.12}$$

$$\hat{n}^\alpha = \frac{1}{\sqrt{2}}\left(n^\alpha - u^\alpha\right), \tag{4.13}$$

$$m^\alpha = \frac{1}{\sqrt{2}}\left(v^\alpha + i w^\alpha\right). \tag{4.14}$$

The triad vectors, in turn, are constructed by applying a Gram-Schmidt orthogonalization to the coordinate triad

$$u^i = [x,\ y,\ z], \tag{4.15}$$

$$v^i = [xz,\ yz, -x^2 - y^2], \tag{4.16}$$

$$w^i = \epsilon^i{}_{mn} v^m w^n. \tag{4.17}$$

There remains some freedom in starting the orthogonalization with u, v or w and different implementations have been used by the community. So far, the choice does not seem to have a notable impact on the resulting waveforms.

The approximative character of the tetrad makes it necessary to extract gravitational waves at a sufficiently large distance from the strong field region near the black holes. In practice, extraction radii of the order of 100 $M_{\rm ADM}$ are used in most current simulations. A more general discussion of various issues in the standard wave extraction procedure is given by Lehner and Moreschi [199]. Methods for approximating the Kinnersley tetrad more systematically have been investigated in [54, 230, 231, 229], but have not yet been incorporated into the current generation of black-hole codes.

The energy and linear and angular momentum radiated in the form of gravitational waves is given in terms of the Newman-Penrose scalar Ψ_4 via the integrals (see, e.g. [97, 257])

$$\frac{dE_{\rm rad}}{dt} = \lim_{r\to\infty}\left(\frac{r^2}{16\pi}\int_\Omega\left|\int_{-\infty}^t \Psi_4 d\tilde{t}\right|^2 d\Omega\right), \tag{4.18}$$

$$\frac{dP_{i,\rm rad}}{dt} = -\lim_{r\to\infty}\left(\frac{r^2}{16\pi}\int_\Omega \hat{\ell}_i\left|\int_{-\infty}^t \Psi_4 d\tilde{t}\right|^2 d\Omega\right), \tag{4.19}$$

$$\frac{dJ_{i,\rm rad}}{dt} = -\lim_{r\to\infty}\frac{r^2}{16\pi}\mathrm{Re}\oint \hat{J}_i\left[\int_{-\infty}^t\left(\int_{-\infty}^{\tilde{t}}\Psi_4 d\bar{t}\right)d\tilde{t}\right]\left(\int_{-\infty}^t \Psi_4 d\tilde{t}\right)d\Omega, \tag{4.20}$$

where

$$\hat{\ell}_i = [-\sin\theta\cos\phi,\ -\sin\theta\cos\sin\phi,\ -\cos\theta], \tag{4.21}$$

$$\sin\theta\hat{J}_x = -\sin\theta\sin\phi\partial_\theta - \cos\theta\cos\phi\partial_\phi + is\cos\phi, \tag{4.22}$$

$$\sin\theta\hat{J}_y = \sin\theta\cos\phi\partial_\theta - \cos\theta\sin\phi\partial_\phi + is\cos\phi, \tag{4.23}$$

$$\hat{J}_z = \partial_\phi, \tag{4.24}$$

and $s = -2$ is the spin weight.

In practice, the integrals are evaluated on coordinate spheres with radius $r_{\rm ex}$ where one also calculates Ψ_4. The errors arising from the use of finite radii can be estimated by calculating the quantities at different extraction radii and studying the variation of Ψ_4 and the momenta analogous to a convergence study of the code's performance at different grid resolutions. The uncertainties depend on the details of the simulation, but in general are of the order of a few percent or less for extraction radii of the order of $10^2\ M_{\rm ADM}$ (see e. g. [78, 278]).

An alternative method for extracting gravitational waves is based on the Zerilli-Moncrief formalism [306, 227] and provides the GW signal in the form of two gauge invariant perturbation functions. More details about this method and applications can be found in [8, 7, 280, 192] and references therein.

Chapter 5

A brief history of black hole simulations

Attempts at solving the Einstein equations numerically date back to the 1960s and 1970s and the pioneering work by Hahn, Lindquist, Eppley, Smarr and coworkers [158, 127, 271, 273, 272]. These early attempts focused on initially time symmetric, spacetimes in axisymmetry and were therefore restricted to head-on collisions of black holes. The resulting simulations turned out to be relatively short-lived, however, compared with the dynamic timescale of the problem. Considering that modern supercomputers are just about powerful enough to facilitate numerical simulations of black-hole binaries, it is clear, that the early numerical studies were inhibited by the computational resources available at the time.

It was therefore more than a decade later, before the significant increase in computer power led to a systematic reinvestigation of the problem in the framework of the "Grand Challenge" (see e. g. [25, 26, 27, 38, 113, 21]). These studies predicted a total radiation of the order of $10^{-3}M_{\rm ADM}$ emitted in the head-on collision of two black holes [26]. Simulations of unequal-mass binaries revealed a gravitational recoil or kick of up to $10-20$ km/s [21]. Simulations were also performed for the first time in three dimensions [23]. In spite of this progress, however, the fundamental difficulties with instabilities in the numerical simulations was not overcome. After the end of the Grand Challenge, a joined effort by the universities of Pittsburgh, Penn State and Texas investigated grazing collisions using the black hole excision method [80].

The 1990s also saw the first investigation of alternative ways to write the Einstein equations. Bona and Massó wrote the evolution equations in the form of balance laws [66, 67, 68], not dissimilar to the way the equations of hydrodynamics are commonly implemented numerically. Even though their efforts did not overcome the stability problems, the idea of using alternative formulations was gradually adopted by other groups and eventually provided a major ingredient in solving the binary black-hole problem (cf. Sec. 3.1). Most importantly, test simulations using the BSSN formulation [267, 51] demonstrated improved stability properties.

The BSSN system also played an important role in the studies of the numerical relativity group of the Albert Einstein Institute in Potsdam starting in the late 1990s. These efforts used initial data of puncture type, factored out the Brill-Lindquist conformal factor during the evolution and employed coordinate conditions which keep the black hole centers fixed on the numerical grid. These studies resulted in the first grazing collisions of black holes [84], the first use of mesh-refinement in black hole simulations [83] and the first long-term stable simulations of black-hole head-on collisions [17] as well as single black hole spacetimes [15]. A guiding principle for many of these studies was to absorb as much as possible the dynamics of the system in the coordinates and use gauge conditions which drive the system into quasi-stationarity. Eventually, this approach led to simulations of orbiting binaries on time scales similar to the orbital period [87, 123].

In view of the persistent stability problems, the Lazarus project attempted to use fully non-linear evolutions until shortly before the merger of the binary, but then match the evolution to a perturbative treatment (see [34, 36] and references therein). This approach facilitated the evolution of relatively short, plunging configurations and provided estimates on the gravitational recoil [96] as well as the first results on spinning binaries [37].

By early 2005, the combined methods of the BSSN formulation, improved gauge conditions and/or black hole excision allowed the community to study head-on collisions of black holes using mesh-refinement, more accurate fourth order numerical schemes and/or non-conformally flat initial data of Kerr-Schild type [133, 280, 307].

The year 2005 also saw the eventual breakthrough, when Pretorius used the remarkable combination of the generalized harmonic formulation of the Einstein equations, implicit numerical schemes and spatial compactification to provide the first simulation of a binary through inspiral and merger [248]. About half a year later, the groups at Brownsville and Goddard independently discovered a method to evolve and merge black-hole binaries of puncture type using a relatively straightforward to implement generalization of previous puncture evolutions with the BSSN system [98, 41]. Retrospectively, it is quite remarkable that these two notably different methods have provided within a few months a successful path to the "holy grail of numerical relativity". As of 2008, there exist about ten independent numerical codes of one or the other method which have been demonstrated to produce stable and convergent simulations of at least some types of black-hole binary spacetimes [249, 40, 100, 169, 278, 86, 262, 282, 192, 128]

In the next section we will summarize the results obtained with these codes in the course of the last two and a half years.

Chapter 6

Properties of black-hole binaries

The majority of published articles forming the core of this thesis are concerned with numerical simulations of black-hole binaries and the extraction of physical results from those evolutions. Those numerical simulations have been performed with the MAYA code developed at Penn State University [270], Sperhake's LEAN code [278] and Brügmann's BAM code [86]. In each case, the code used is specified explicitly.

Performing numerical simulations of general binary spacetimes has only become possible in the last few years following the breakthroughs of 2005. The results presented in the articles are best viewed in the context of the improved understanding of black-hole binaries as developed by the relativity community as a whole. In this section we therefore provide as background a summary of numerical results on the dynamics of black-hole binaries pertaining to astrophysics, the ongoing effort to detect gravitational waves and fundamental physics. Further details on all studies are given in the references cited in the course of this section. More details on the author's work as presented in this thesis is given in the set of published articles attached below.

Following the breakthroughs of 2005, the numerical relativity community has generated a wealth of results on black-hole binary spacetimes. In order to present these results, it is instructive to discuss the units commonly used in the modeling of black holes. We have already mentioned that the speed of light c and the gravitational constant G are set to unity throughout this work. This choice can be used to relate cgs units, commonly used in astrophysics, according to

$$1 \text{ s} = 2.9979 \times 10^{10} \text{ cm}, \tag{6.1}$$

$$1 \text{ g} = 7.4237 \times 10^{-29} \text{ cm}. \tag{6.2}$$

It is quite natural, in consequence, to use but one of these units to express dimensional physical quantities in general relativity. For example, we can write the mass of the sun as

$$M_\odot = 1.989 \times 10^{33}\ \mathrm{g} = 1.477\ \mathrm{km} = 4.923 \times 10^{-6}\ \mathrm{s}. \tag{6.3}$$

We can thus easily compare the mass of the sun $M_\odot = 1.477$ km with the solar radius $R_\odot = 6.960 \times 10^5$ km and see that the sun is an object well described by Newtonian gravity.

In the case of black hole spacetimes, we have a further simplification in that such spacetimes are scale invariant. In Sec. 3.3 we have summarized the physical parameters of generic black-hole initial configurations. In particular, we noted that the total ADM mass of the system merely represents a scaling factor in a numerical simulation. That is, expressed in units of the ADM mass, all quantities of a simulation have the same numerical value irrespective of the magnitude of the mass itself. A single numerical simulation thus represents a one-parameter family of solutions. A further consequence is that dimensional quantities are commonly expressed in units of the black hole mass M or the ADM mass of the system M_{ADM}. The conversion to cgs or SI units is straightforward, however, once the mass is specified, for example as $10\ M_\odot = 14.77$ km $= 4.923 \times 10^{-5}$ s.

While the total mass of the system does not affect a numerical simulation, we emphasize, that it is important for the interpretation of the results from the viewpoint of gravitational wave detection. Suppose, a characteristic frequency is given by $\omega = C/M_{\mathrm{ADM}}$, with C some constant. The maximal sensitivity of the LIGO detector is located in a window around 150 Hz. The ADM mass of the system will determine the system's characteristic frequency and thus where this frequency is located in the LIGO sensitivity range. For the case of a binary of two non-spinning holes of mass 5 $M_\odot$ each it is the earlier inspiral phase which falls into the maximum sensitivity range of LIGO, whereas for a system of two black holes of mass 50 $M_\odot$, it is the merger and ringdown signal. This is illustrated in Fig. 4 of Pan et al. [238].

In gravitational wave data analysis, there exist further parameters which describe the location of the black-hole binary relative to the earth: the source's position on the sky and its inclination relative to the plane of the detector. These parameters are not related to the physical properties of the binary, however, and need not concern us in this work.

6.1 Non-spinning, equal-mass binaries

The inspiral of two non-spinning black holes of equal mass represents the simplest binary configuration and has been the first to be evolved successfully through inspiral, merger and ringdown [247, 41, 98]. This scenario is currently the best understood type of binary systems and we will use it here to also illustrate the fundamental characteristics of a black-hole inspiral and merger and the resulting waveform patterns.

In realistic astrophysical scenarios, the binary will complete thousands of orbits or more before coalescence. Unless there is significant interaction with third party objects, the binary will loose all orbital eccentricity due to the circularizing effect of gravitational wave emission [241]. Numerical simulations are currently able to simulate only a few tens of orbits by which time most binaries are expected to be in quasi-circular configuration. In order to accurately model such systems, numerical simulations need to start from initial data which represent as closely as possible a snapshot of a binary in quasi-circular inspiral. In practice, this has commonly been approximated in one of the three methods we discussed in Sec. 3.3. All of these methods, however, result in measurable eccentricity in the orbits (see, for example, [90, 44, 243, 180]). This small residual eccentricity is a major source of uncertainty in the comparison of numerical with post-Newtonian results [78] and improved methods to further reduce the eccentricity have been designed using iterative procedures [243, 78] or the integration of post-Newtonian equations over a larger number of orbits [180].

For illustration of the binary inspiral, we show in the upper panel of Fig. 6.1 the puncture trajectories of the holes as obtained for the simulation of a relatively short inspiral starting from the so-called R1-configuration (see Table I of [40]). For trajectories containing more orbits, see, for example, Fig. III of [78]. One of the most remarkable features of both, moving punctures as well as evolutions using the generalized harmonic formulation is the similarity of the black hole coordinate trajectories with the intuitively expected picture. In fact, the gravitational wave signal obtained from using the coordinate trajectory of the apparent horizon in the quadrupole formula for GW emission [241] shows remarkable agreement with the wave signal extracted from the numerical simulation (see e. g. Fig. 7 of [90]. Bearing in mind the gauge dependence of the trajectories, this result was by no means to be expected.

Even though Fig. 6.1 shows a relatively short inspiral, it illustrates the three phases commonly used to describe a binary evolution. First, however, we note the

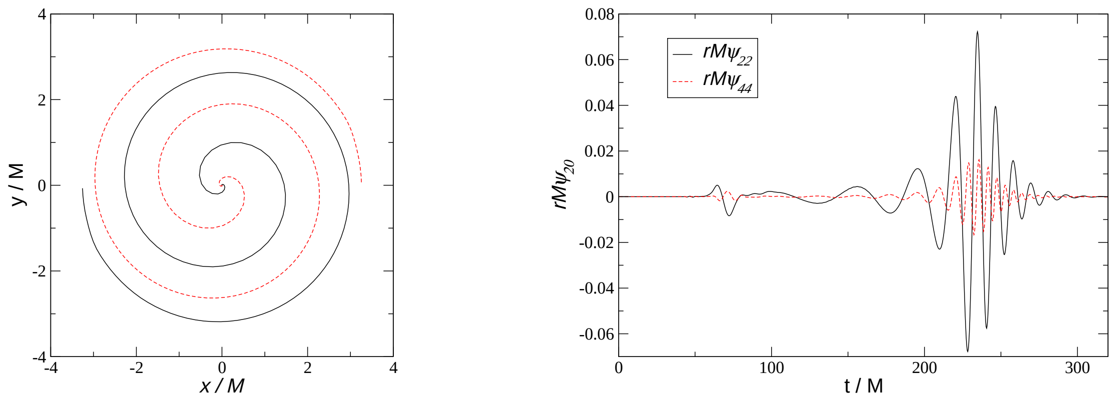

Figure 6.1: Upper panel: Trajectories of the two holes in the inspiral of two equal-mass, non-spinning holes starting from a coordinate separation $d/M = 6.514\ M$ (see entry R1 in Table I of [40]. Lower panel: The $\ell = 2$, $m = 2$ mode of the Newman-Penrose scalar Ψ_4 extracted from the same simulation at radius $r_{\rm ex} = 60\ M$.

small pulse near $t = 70\ M$. This pulse is an unphysical artifact of the approximative nature of the initial data as described in Sec. 3.3. Starting at around $t = 100\ M$ we see a few cycles with relatively long wavelength which are generated in the inspiral. The large amplitude part of the waveform between approximately 210 and 240 M represents the plunge and merger stage and the remainder is the so-called ringdown of the merged hole. Here, the signal is closely approximated by an exponentially damped sinusoid.

Our example in Fig. 6.1 also illustrates the relatively smooth transition from the inspiral to the ringdown and is representative for simulations performed by other groups. This smooth transition is taken advantage of in the effective one body approach (EOB) [91, 93] which employs analytic tools to approximately bridge the gap between the post-Newtonian methods used to model the inspiral and the close-limit ring-down part of the waveform modeled by perturbation theory. The EOB approach is given flexibility in the form of free parameters which has enabled it to reproduce numerical results with an accuracy significantly higher than the numerical accuracy [120, 121] (see also [122] for the corresponding study of unequal mass binaries).

The accuracy of numerically generated waveforms is likely to play a crucial role in their eventual use in gravitational wave observations. Uncertainties in the numerical results arise from various sources. Those errors arising from numerical limitations, as for example discretization error, outer boundary effects and wave extraction at finite radii, can be assessed rather straightforwardly, e. g. convergence analysis, extraction at different radii etc. The impact of the initial data, however, represents a more challenging problem, because different initial data types require different evolution methods. As a first step, orbital simulations starting from Cook-Pfeiffer excision and puncture data have been compared in [39] and showed qualitatively good agreement. A more detailed comparison is currently inhibited by residual spin in the excision data. Such problems are not present in comparisons of head-on collisions of black-hole binaries. The comparison of collisions starting from Brill-Lindquist, Misner and superposed Kerr-Schild data exhibit good quantitative agreement [278]. Minor differences, of the order of a few per cent in radiated energy, in the evolutions of Kerr-Schild data might be attributed to spurious radiation present in these data [63]. In summary, these results are reassuring, though more detailed comparisons will be needed in the future.

All simulations of the last orbit of equal-mass, non-spinning binaries agree rather well on the total radiated energy and angular momentum in the course of the inspiral, merger and ringdown. About 3.5 % of the total mass and about 21 % of the total angular momentum of the binary system are carried away in the form of gravitational waves. Contributions from the earlier stages of the inpiral have been estimated to radiate a further 1.5 % of the total mass (see e. g. [91]). The radiation is dominated by the $\ell = 2$, $m = \pm 2$ quadrupole contribution which carries > 98 % of the total radiated energy [40, 100, 278, 86, 59]. This is illustrated in the upper panel of Fig. 6.1 where we show the $\ell = 2$, $m = 2$ mode as well as the next strongest mode $\ell = 4$, $m = 4$. From Eq. (4.18) we see that the energy scales with the square of the wave amplitude and it becomes clear that only a small fraction of the energy is contained in $\ell = 4$, $m = 4$. All other modes are negligible compared with these two.

The dominant role of the quadrupole radiation is no surprise and directly follows from post-Newtonian studies (see [61] and references therein). Indeed, most of the inspiral phase up to about the last few orbits is rather well described by the post-Newtonian approximation and one of the most important questions facing the community right now is to determine, how close to the merger the PN approximation breaks down. For this comparison it is often convenient to split the complex Newman-Penrose scalar Ψ_4 into phase and amplitude

$$\Psi_4(t) = A(t) e^{i\phi(t)}. \tag{6.4}$$

Sometimes, the wave signal is also expressed in terms of the gravitational wave polarizations + and × related to Ψ_4 according to [1]

$$\Psi_4 = \partial_t \partial_t (h_+ - i h_\times), \tag{6.5}$$

and the amplitude phase decomposition is applied to h_+ and $h_\times$. The Newman-Penrose scalar is the standard choice of describing gravitational waves in numerical relativity, whereas h_+ and $h_\times$ are more directly related to the displacements in gravitational wave detectors and thus more popular in GW data analysis. For the comparison between numerical and post-Newtonian results, the choice of variables is not important, however.

First comparisons between numerical and PN results demonstrated that the PN-adiabatic model agrees better with the numerical results at larger BH-separations, but gives reasonable results even when extrapolated to the formation of a common apparent horizon [90]. This study also found the highest 3PN and 3.5PN order to result in the best agreement with the numerical data. A study using numerical waveforms covering the last 14 cycles of the inspiral was presented in [44, 43] and revealed an accumulated phase discrepancy of about 1 rad until shortly before the merger. Subsequent numerical simulations using improved initial data and higher order finite differencing [179] or spectral methods resulted in even better agreement [164, 78]. The most comprehensive comparison performed by the Caltech group [78] showed a phase difference between numerical and various PN waveforms of about 0.1 rad. The particularly good agreement observed for the Taylor T4 approximant result appears to be more coincidental, as it is significantly smaller than the discrepancies among the different PN results. Comparisons with post-Newtonian results uniformly found higher order amplitude corrections to the PN waveforms to improve the agreement with numerical results [90, 164, 78].

So far we have focused on quasi-circular binaries. While the majority of systems are indeed expected to have vanishing eccentricity, some astrophysical scenarios, as for example third body interactions, may induce eccentric orbits. The effect of significant eccentricities on the dynamics of the binary and the gravitational wave signal has been studied in [279, 172]. Relatively small eccentricities cause a small increase in the radiated energy and angular momentum, whereas binaries with large eccentricities plunge rather than inspiral which significantly reduces the energy and momentum emission. Binaries with larger eccentricity also emit an increasing fraction of their energy in the $\ell = 2$, $m = 0$ mode as opposed to the dominating $\ell = 2$, $m = \pm 2$ modes. The results obtained so far indicate, that there

[1] see [59] for a discussion of the constants of integration

exists a relatively sharp distinction between orbiting and plunging configurations: simulations with orbital angular momentum $L \lesssim 0.8M^2$ plunge, those with $L \gtrsim 0.8\ M^2$ inspiral. Hinder *et al.* [172] also demonstrated that the GW merger signal shows universality for angular momenta above the critical value.

A remarkable behavior of black-hole binaries has been found by Pretorius [251] when fine tuning the linear momentum parameter of the holes in the initial data. Such fine tuning leads to binaries which exhibit "zoom-whirl" behavior, that is, they inspiral initially, but then may stall at some finite separation for a while and eventually merge or separate. A similar behavior is known in the structure of geodesics of single black hole spacetimes. Similar black-hole encounters were studied by Washik et al. [296] who show that the maximum spin parameter of the final hole resulting from such mergers is $a/M \lesssim 0.78$ and is obtained for orbital angular momentum $L \sim M^2$.

6.2 Unequal mass binaries

Spacetimes containing black-hole binaries of unequal mass are no longer symmetric under rotations by 180 degrees around the axis defined by the orbital angular momentum. This loss of symmetry has important consequences for the gravitational wave emission. In particular, the radiation of linear momentum is no longer isotropic and results in a net-loss of linear momentum of the binary system. By conservation of linear momentum, this imparts a recoil or kick on the final merged hole. At the leading order, this effect arises from the overlap of the mass-quadrupole with the octupole and flux-quadrupole moments [72, 240, 55]. This kick is a genuinely relativistic effect and has significant repercussions on astrophysical systems containing black holes [75, 159, 209, 219, 295, 200, 71, 174, 153, 236, 292, 204]. It might also manifest itself directly in astrophysical observations of quasi-stellar objects without host galaxies [157, 211, 173, 220, 205] or the distorted morphology of $\times$-shaped radio sources [217, 209, 219].

The kick generated by the inspiral and merger of unequal mass binaries has been the subject of various approximative studies [134, 135, 130, 62, 115, 275, 276], but highly accurate results require the solution in the framework of fully non-linear general relativity and, thus, numerical relativity. First numerical studies of certain mass ratios revealed kick velocities of the order of 100 km/s [169, 42]. In order to find the maximum kick resulting from unequal-mass binary inspiral, González *et al.* [147] calculated the kick for mass ratios ranging from $q \equiv M_1/M_2 = 1$ to $q = 4$ and found a maximum kick of 175 ± 11 km/s for the mass ratio $\eta \equiv q/(1+q)^2 = 0.195 \pm 0.005$.

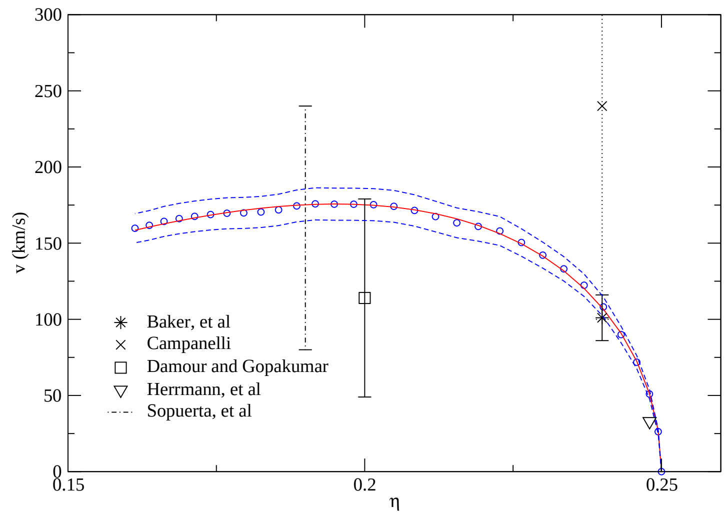

Figure 6.2: The recoil velocity resulting from the inspiral and merger of a non-spinning binary with mass ratio $\eta = M_1 M_2/(M_1+M_2)^2$ as calculated in [147]. For comparison the figure also includes values from Refs. [96, 169, 42, 115, 275].

This is illustrated in Fig. 6.2. The recoil as function of η is well modeled by Fitchett's [134] formula

$$v = A\eta^2\sqrt{1-4\eta}(1+B\eta), \tag{6.6}$$

with the coefficients $A \approx 1.2\times 10^4$ and $B \approx -0.93$ [147]. This velocity is larger than the escape velocities of about 30 km/s for globular clusters and falls into the range of escape velocities predicted for dwarf galaxies, but is significantly smaller than that from giant elliptic galaxies of the order of 1000 km/s [219]. The resulting ejection or displacement of the black hole following a merger has important repercussions on models for the formation history of black holes as well as the structure of host galaxies and the population of intergalactic black hole populations (see e. g. [75, 219, 295, 159, 236]).

In contrast to the emission of linear momentum, the radiated energy and angular momentum is maximal in the equal mass case. Radiated energy and the final spin parameter of the single hole are well approximated by fitting formulas [147, 59]

$$E_{\rm rad} = 0.0363\ M\left[\frac{4q}{(1+q)^2}\right], \tag{6.7}$$

$$j_{\rm fin} = 0.089 + 2.4\frac{q}{(1+q)^2}. \tag{6.8}$$

A further consequence of the reduced symmetry of unequal-mass binaries is the more complex structure of higher order multipoles. In the equal-mass case, all radiation modes with odd m vanish by symmetry. For unequal masses, this is no longer the case and the second strongest mode is typically $\ell = 3$, $m = \pm 3$. Additionally, it turns out that the percentage of energy radiated in higher ($\ell > 2$) modes increases from less than two per cent for $q = 1$ to more than 10% for $q = 4$. This is illustrated in Fig. 12 of [59]. This sensitivity of higher order modes to the mass ratio is significant for gravitational wave data analysis because the inclusion of higher order modes in the analysis is likely to improve the accuracy of parameter estimates and the detection range of gravitational wave observations (see e. g. [31, 32]).

The comparison of numerical with post-Newtonian results for unequal-mass binaries represents a more challenging task, because of the increased computational cost of numerical simulations as the mass ratio q deviates more strongly from 1. There are currently not as accurate and long numerical waveforms available for the comparison. The sequence of unequal-mass binaries generated for the kick calculations in [147] was used in Berti *et al.* [59] for a comparison with post-Newtonian results in the inspiral and black-hole quasi-normal mode studies (see [105, 197, 191, 57] and references therein for an introduction to quasi-normal modes) in the ring down phase. Similar to the equal-mass study in [90], post-Newtonian results were found to predict remarkably well the relation between wave frequency and amplitude. The convergence of the PN series is non-monotonic but the inclusion of higher order terms improves the agreement with the numerical results. Spin and mass parameter estimates obtained from the black hole ring down are in excellent agreement with the values derived from the measured gravitational radiation and balance arguments. Intriguing oscillations observed in the quality factor estimates obtained in the ring down phase could indicate non-linear effects but might also be artifacts of numerical noise. Simulations of higher accuracy are required to conclusively address this issue.

The first study on the use of numerically generated waveforms in gravitational wave data analysis was performed by Baumgarte *et al.* [47]. They discuss sources of uncertainties in using numerical waveforms and estimate that first detection efforts will require about 100 templates to cover the zero-spin part of the parameter space. Pan *et al.* [238] used a set of numerical waveforms of equal and unequal-mass binaries and studied the agreement of the numerical waveforms with a variety of PN template families. For this study they used the fitting factor (FF) [29] which takes into account the instrumental sensitivity and is a standard tool in matched filtering data analysis. They thus found good agreement with FF ≥ 0.96 for total masses of $10 - 20\ M_\odot$ and ground-based detectors. For larger masses of the binary, the detectors become increasingly sensitive to the merger and ringdown part of the waveform, but the addition of a phenomenological 4PN term extends the range of high fitting factors to about 120 $M_\odot$. The EOB method as well as the phenomenological Buonanno-Chen-Valisneri [89] family of waveforms similarly leads to high fitting factors in in the mass range $10 - 120$ $M_\odot$. The EOB approach is compared in further detail with numerical simulations in Buonanno *et al.* [93], where the addition of a 4PN term is shown to result in phase agreement within 8 % of a GW cycle at the end of the ring down phase. The EOB method was also used by Damour and Nagar [119] to compare the predictions for the spin of the final merged hole. Agreement of about 2 % with the numerical results was found. We have already mentioned the study in [122] which uses the EOB method to fit numerically generated waveforms of unequal-mass binaries to within tiny phase differences.

The generation of phenomenological waveforms is the subject of Refs. [10, 11]. Hybrid waveforms obtained from matching numerical with PN waveforms are used to create a parameterization of unequal mass inspiral waveforms and study their use in GW data analysis. The results indicate that the detection range of ground-based interferometers might be enhanced significantly by using such waveform families.

A particular type of binaries of relevance for gravitational wave physics are the so-called extreme mass ratio inspirals (EMRI) consisting of a stellar size compact object orbiting around a supermassive black hole. EMRIs are considered one of the most important sources of the space interferometer LISA (see e. g. [175, 176]). Mass ratios of $q \sim 10^{-6}$ characteristic of such systems are currently beyond the range of capabilities of numerical relativity and the modeling of these scenarios is commonly done in the framework of perturbation theory and self force calculations (see [245] for a review). Numerical results might still be of interest for less extreme mass ratios, as simulations with $q = 10$ appear to be feasible and their comparison with approximative studies might allow for some calibration of the methods analogous to the comparison between numerical and PN results.

6.3 Spinning binaries

Spinning binaries are by far the most complex black-hole binaries. Bearing in mind, that six out of the seven free physical parameters determine the spin, this is not surprising. Indeed, the resulting parameter space is so large, that only a subset has been studied in any detail so far. The majority of work has gone into studying binaries where the spins are aligned or anti-aligned with the orbital angular momentum. The case of the spin being aligned with the orbital angular momentum may also be the astrophysically most likely scenario as accretion processes have been argued to result in alignment of spin and orbital angular momentum [64].

A particularly intriguing question concerns the formation of naked singularities as would be the case for Kerr holes with spin parameter $a/M \geq 1$. In particular, spins aligned with the orbital angular momentum might be suspected to lead to a very large spin of the final merged hole. The simulations presented in Ref. [99] (see also [246]), however, demonstrate the difficulties in creating a maximally spinning black hole in this way. The larger the spin magnitude, the longer the inspiral lasts and the more angular momentum and energy is radiated from the system before merger. For the interpretation of this delayed inspiral it is helpful to consider the innermost stable circular orbit (ISCO) [189, 109, 91, 48, 117, 244, 60, 116, 151]. In particular, it can be shown that the ISCO separation decreases for binaries with aligned spins and increases for spins anti-aligned with the orbital angular momentum [244]. Assuming that the ISCO gives a measure for the merger separation, this result agrees with the delayed and accelerated inspiral observed for aligned and anti-aligned inspirals respectively.

Binaries with spins which are not parallel to the orbital angular momentum exhibit spin-precession. Campanelli *et al.* [102, 103] studied the precession using configurations where the spins are either in the orbital plane or oriented at 45 degrees relative to the plane. They use a simplified method to determine the spin of the individual holes where they integrate the flat space Killing vectors over the horizon surface. Their simulations demonstrate the precession of the individual spins as well as the realignment of the spin of the final black hole, the so-called spin-flip, which may explain the reorientation of jets observed in radio galaxies [239, 196]. The spin-orbit interaction was studied in special configurations starting either without spin but with orbital angular momentum or the other way round in [101]. In both cases the result is a transfer of momentum from spin to orbit or vice versa. This coupling also contributes to the generally more complex structure of spinning binaries.

An effect we have already discussed in the context of unequal-mass binaries, is the recoil or rocket effect in binary black hole mergers. Post-Newtonian studies predicted contributions to the recoil arising from the spin-spin and spin-orbit coupling in black-hole binaries [186]. One of the most surprising results as yet obtained from numerical simulations of black-hole binaries is the magnitude of the recoil in spinning binaries. The first studies focused on spins parallel to the orbital angular momentum and anti-aligned with each other. These scenarios generate kicks of up to 500 km/s [170, 103, 192] for inspirals and some tens of km/s for head-on collisions [106]. Even larger kicks of up to $1,300$ km/s were predicted by [103] for configurations with spins in the orbital plane, but pointing in opposite directions. Subsequent numerical studies of this scenario revealed unexpected kick magnitudes of about $2,500$ km/s for spin amplitudes $a/M \approx 0.7$ which implies maximum values of $4,000$ km/s extrapolated for $a/M \to 1$ [103, 146, 104]. Kicks above 1000 km/s are also predicted by the EOB model [264]. Such large recoil velocities would in fact be sufficient to eject black holes even from giant elliptic galaxies. Given that galaxies with bulges appear to ubiquitously harbor supermassive black holes [132], it appears that these "superkicks", while theoretically possible, are not realized very often in actual galactic mergers. This is also indicated by the Monte Carlo study employing the EOB model by Schnittman *et al.* [264] which predicts that only a few percent of mergers with mass ratios $1 \leq q \leq 10$ and spin magnitude $a_1 = a_2 = 0.9$ with random spin orientation results in kicks above 1000 km/s.

The surprising magnitude of the recoil for spinning configurations has sparked a wealth of more detailed investigations and attempts to generate fitting formulas valid for general types of initial configurations. A multipolar analysis of the recoil was presented Schnittman *et al.* [265] for unequal masses and non-zero and non-precessing spins. Including specific multipoles with $\ell \leq 4$ was found to determine the kick within a few percent, higher order multipoles being almost negligible. This is in agreement with numerical studies which show the kick to be dominated by overlaps between low multipoles [170, 246]. Schnittman *et al.* further found these multipoles to describe well, how the kick is built up during the inspiral and merger, including breaking effects in the late stages. The numerical results were found to be well reproduced by an "effective Newtonian" formula. A heuristic formula suggested in Campanelli *et al.* [103] for the kick magnitude was tested by Lousto and Zlochower [206] using numerical simulations of three families of unequal-mass, spinning binaries. They observe good agreement between the model and the numerical simulations and find most of the kick to be generated close to the merger of the holes. The most recent investigation by Baker *et al.* [45], however, called into question the kick magnitude for unequal masses. In particular, they observe a dependence on η^3 instead of η^2 which implies fewer kicks above 1000 km/s, though still more than the number predicted by the EOB study of Schnittman and Buonanno [264]. The dependence of the kick on the orientation angle of the spin in the initial orbital plane was systematically analyzed in [171, 85]. The sinusoidal dependence is in agreement with the heuristic model of [103]. This dependence of the recoil on the spin-orientation can be understood intuitively in terms of frame dragging (see Sec. IV C 2 and in particular Fig. 5 in [252]). The key idea is that the two holes exert frame dragging on each other and thus generate a periodic motion of the line connecting the holes in the direction of the orbital angular momentum. The frame dragging is terminated at merger and the initial spin-orientation determines at which phase of the periodic motion the merger occurs. A further result shown in Brügmann *et al.*[85] is the proportionality of the recoil to the difference in energy emission in the $\ell = 2$, $m = +2$ and $m = -2$ modes. 2.5 Post-Newtonian order predictions were found to accurately model the spin evolution up to about 60 M before the merger, but not beyond that, illustrating the need for more sophisticated models, such as that of [264]. The asymmetry in the quadrupole radiation of these superkick also implies that such GW sources appear brighter in some directions than others. Implications of spinning binaries for GW detection were also investigated by Vaishnav *et al.* [291]. They calculate the match between waveforms resulting from different spinning binary configurations and find the inclusion of higher order multipoles necessary to break the degeneracy between the waveforms in the context of matched filtering analysis.

Comparisons of PN predictions with numerical results for the emitted gravitational waveforms from spinning binaries are currently restricted to the case of spins aligned with the orbital angular momentum. First results indicate that these scenarios might be modeled by PN theory with comparable accuracy as in the non-spinning case [163]. There still remains a lot of work to do before more comprehensive statements can be made.

A question of significant astrophysical interest concerns the spin-distribution arising from black hole mergers. This effect was investigated in a series of papers by Rezzolla *et al.* [254, 255, 256] which provided semi-analytic fits. An analytic study based on conservation of momentum was presented by Boyle *et al.* [77, 76] and suggests a series of numerical simulations to nail down remaining free parameters in their predictions. The analytic study by Buonanno *et al.* [92] pointed out a particularly intriguing scenario: the generation of a non-spinning hole in a merger of a binary with spins anti-aligned with the orbital angular momentum. According to their model, this special case can only be realized in the case of unequal masses. The fitting formulas of [254] as well as numerical simulations presented in Berti *et al.* [58] agree remarkably well with the study of [92].

Chapter 7

Conclusions

In summary, numerical relativity has achieved what has for a long time been called its "holy grail": The simulation of a black-hole binary through inspiral and merger. The methods used for this breakthrough have turned out to be remarkably robust and have so far been applied with great success to a wider class of black-hole binaries. In the course of the last few years, numerical relativity has thus produced important results for astrophysics, including kicks and diagrams for the spin distribution of black holes. At the same time, the field has established a connection with approximative theories. The good agreement with PN results is encouraging from the point of view of generating hybrid waveforms for use in gravitational wave detection and parameter estimates. The use of numerical waveforms in the data analysis pipeline is currently being started and is widely expected to improve the detection range even of the current generation of GW detectors. Numerical relativity has also opened the door to studying a variety of fundamental questions such as the existence of zoom-whirl orbits and testing the cosmic censorship conjecture.

In spite of the dramatic progress of the field, many open questions remain. Most outstanding among these are a more systematic investigation of the spin parameter space including calibration of the results versus approximative theories. The accuracy of the simulations performed to date has probably been higher than anticipated, but it remains to be seen, whether it will prove sufficient for the daunting task to generate complete waveform template banks for the ongoing effort to detect and observe gravitational waves. It will also be interesting to probe a larger range of parameters, as for example the mass ratio or the kinetic energy of binary spacetimes and compare results with analytic or perturbative predictions. Questions such as these will keep the community busy for years to come and it remains to be seen, how many surprises are still to be discovered in the dynamics of black-hole binaries.

Bibliography

[1] Carpet Code homepage: `http://www.carpetcode.org/`

[2] Cactus Computational Toolkit homepage: `http://www.cactuscode.org/`

[3] Samrai homepage

[4] openGR homepage

[5] HAD homepage

[6] Abbott, B. ; LIGO Scientific Collaboration the: LIGO: The Laser Interferometer Gravitational-Wave Observatory. (2007). – arXiv:0711.3041 [gr-qc]

[7] Abrahams, A. ; Bernstein, D. ; Hobill, D. ; Seidel, E. ; Smarr, L.: Numerically generated black-hole spacetimes: Interaction with gravitational waves. In: *Phys. Rev. D* 45 (1992), S. 3544–3558

[8] Abrahams, A. M. ; Evans, C. R.: Gauge-invariant treatment of gravitational radiation near the source: Analysis and numerical simulations. In: *Phys. Rev. D* 42 (1990), S. 2585–2594

[9] Acernese, F. u. a.: Status of VIRGO. In: *Class. Quantum Grav.* 22 (2005), S. S869–S880

[10] Ajith *et al.*, P.: Phenomenological template family for black-hole coalescence waveforms. In: *Class. Quantum Grav.* 24 (2007), S. S689–S700. – arXiv:0704.3764 [gr-qc]

[11] Ajith *et al.*, P.: A template bank for gravitational waveforms from coalescing binary black holes: I. non-spinning binaries. In: *Phys. Rev. D* 77 (2008), S. 104017. – arXiv:0710.2335 [gr-qc]

[12] Alcubierre, M.: Hyperbolic slicings of spacetime: singularity avoidance and gauge shocks. In: *Class. Quantum Grav.* 20 (2003), S. 607–624. – gr-qc/0210050

[13] Alcubierre, M.: Are gauge shocks really shocks? In: *Class. Quantum Grav.* 22 (2005), S. 4071. – gr-qc/0503030

[14] Alcubierre, M. ; Benger, W. ; Bügmann, B. ; Lanfermann, G. ; Nerger, L.: The 3D Grazing Collision of Two Black Holes. In: *Phys. Rev. Lett.* 87 (2001), S. 271103. – gr-qc/0012079

[15] Alcubierre, M. ; Brügmann, B.: Simple excision of a black hole in 3 + 1 numerical relativity. In: *Phys. Rev. D* 63 (2001), S. 104006. – gr-qc/0008067

[16] Alcubierre, M. ; Brügmann, B. ; Diener, P. ; Guzmán, F. S. ; Hawke, I. ; Hawley, S. ; Herrmann, F. ; Koppitz, M. ; Pollney, D. ; Seidel, E. ; Thornburg, J.: Dynamical evolution of quasi-circular binary black hole data. In: *Phys. Rev. D* 72 (2005), S. 044004. – gr-qc/0411149

[17] Alcubierre, M. ; Brügmann, B. ; Diener, P. ; Koppitz, M. ; Pollney, D. ; Seidel, E. ; Takahashi, R.: Gauge conditions for long-term numerical black hole evolutions without excision. In: *Phys. Rev. D* 67 (2003), S. 084023. – gr-qc/0206072

[18] Anderson, A. ; York, J. W. Jr.: Fixing Einstein's Equations. In: *Phys. Rev. Lett.* 82 (1999), S. 4384–4387. – gr-qc/9901021

[19] Anderson, M. ; Hirschmann, E. W. ; Lehner, L. ; Liebling, S. L. ; Motl, P. M. ; Neilsen, D. ; Palenzuela, C. ; Tohline, J. E.: Simulating binary neutron stars: dynamics and gravitational waves. In: *Phys. Rev. D* 77 (2008), S. 024006. – arXiv:0708:2720 [gr-qc]

[20] Ando, M. u. a.: Current status of the TAMA300 gravitational wave detector. In: *Class. Quantum Grav.* 22 (2005), S. S881–S889

[21] Anninos, P. ; Brandt, S.: Head-On Collision of Two Unequal Mass Black Holes. In: *Phys. Rev. Lett.* 81 (1998), S. 508–511. – gr-qc/9806031

[22] Anninos, P. ; Camarda, K. ; Libson, J. ; Massó, J. ; Seidel, E. ; Suen, W.-M.: Finding apparent horizons in dynamic 3D numerical spacetimes. In: *Phys. Rev. D* 58 (1998), S. 024003

[23] Anninos, P. ; Camarda, K. ; Massó ; Seidel, E. ; Suen, W.-M. ; Towns, J.: Three-dimensional numerical relativity: The evolution of black holes. In: *Phys. Rev. D* 52 (1995), S. 2059–2082

[24] Anninos, P. ; Daues, G. ; Massó, J. ; Seidel, E. ; Suen, W.-M.: Horizon boundary condition for black hole spacetimes. In: *Phys. Rev. D* 51 (1995), S. 5562–5578

[25] Anninos, P. ; Hobill, D. ; Seidel, E. ; Smarr, L. ; Suen, W.-M.: Collision of Two Black Holes. In: *Phys. Rev. Lett.* 71 (1993), S. 2851–2854. – gr-qc/9309016

[26] Anninos, P. ; Hobill, D. ; Seidel, E. ; Smarr, L. ; Suen, W.-M.: Head-on collision of two equal mass black holes. In: *Phys. Rev. D* 52 (1995), S. 2044–2058

[27] ANNINOS, P. ; PRICE, R. H. ; PULLIN, J. ; SEIDEL, E. ; SUEN, W.-M.: Head-on collision of two black holes: Comparison of different approaches. In: *Phys. Rev. D* 52 (1995), S. 4462–4480. – gr-qc/9505042

[28] ANSORG, M.: Multi-Domain Spectral Method for Initial Data of Arbitrary Binaries in General Relativity. In: *Class. Quantum Grav.* 24 (2007), S. S1–S14. – gr-qc/0612081

[29] APOSTOLATOS, T.: Search templates for gravitational waves from precessing, inspiralling binaries. In: *Phys. Rev. D* 52 (1995), S. 605–620

[30] ARNOWITT, R. ; DESER, S. ; MISNER, C. W.: The dynamics of general relativity. In: WITTEN, L. (Hrsg.): *Gravitation an introduction to current research*, John Wiley, New York, 1962, S. 227–265. – gr-qc/0405109

[31] ARUN, K. G. ; IYER, B. R. ; SATHYAPRAKASH, B. S. ; SINHA, S.: Higher harmonics increase LISA's mass reach for supermassive black holes. In: *Phys. Rev. D* 75 (2007), S. 124002. – arXiv:0704.1086 [gr-qc]

[32] ARUN, K. G. ; IYER, B. R. ; SATHYAPRAKASH, B. S. ; SINHA, S. ; VAN DEN BROECK, C.: Higher signal harmonics, LISA's angular resolution and dark energy. In: *Phys. Rev.* D76 (2007), S. 104016. – arXiv:0707.3920 [astro-ph]

[33] ASHTEKAR, A. ; KRISHNAN, B.: Isolated and dynamical horizons and their applications. In: *Living Reviews in Relativity* 2004-7 (2004). – [Article in Online Journal] cited on 23 Feb 2001, http://relativity.livingreviews.org/Articles/lrr-2004-10/download/index.html

[34] BAKER, J. ; BRÜGMANN, B. ; CAMPANELLI, M.: Gravitational waves from black hole collisions via an eclectic approach. In: *Class. Quantum Grav.* 17 (2000), S. L149–L155. – gr-qc/0003027

[35] BAKER, J. ; CAMPANELLI, M. ; LOUSTO, C. O.: The Lazarus project: A pragmatic approach to binary black hole evolutions. In: *Phys. Rev. D* 65 (2002), S. 044001. – gr-qc/0104063

[36] BAKER, J. ; CAMPANELLI, M. ; LOUSTO, C. O. ; TAKAHASHI, R.: Modeling gravitational radiation from coalescing binary black holes. In: *Phys. Rev. D* 65 (2002), S. 124012. – astro-ph/0202469

[37] BAKER, J. ; CAMPANELLI, M. ; LOUSTO, C. O. ; TAKAHASHI, T.: The coalescence remnant of spinning binaries. In: *Phys. Rev. D* 69 (2004), S. 027505

[38] BAKER, J. G. ; ABRAHAMS, A. ; ANNINOS, P. ; BRANDT, S. ; PRICE, R. ; PULLIN, J. ; SEIDEL, E.: Collision of boosted black holes. In: *Phys. Rev. D* 55 (1997), S. 829–834. – gr-qc/9608064

[39] Baker, J. G. ; Campanelli, M. ; Pretorius, F. ; Zlochower, Y.: Comparisons of binary black hole merger waveforms. In: *Class. Quantum Grav.* 24 (2007), S. S25–S31. – gr-qc/0701016

[40] Baker, J. G. ; Centrella, J. ; Choi, D.-I. ; Koppitz, M. ; Meter, J. van: Binary black hole merger dynamics and waveforms. In: *Phys. Rev. D* 73 (2006), S. 104002. – gr-qc/0602026

[41] Baker, J. G. ; Centrella, J. ; Choi, D.-I. ; Koppitz, M. ; Meter, J. van: Gravitational-Wave Extraction from an inspiraling Configuration of Merging Black Holes. In: *Phys. Rev. Lett.* 96 (2006), S. 111102. – gr-qc/0511103

[42] Baker, J. G. ; Centrella, J. ; Choi, D.-I. ; Koppitz, M. ; Meter, J. van ; Miller, M. C.: Getting a kick out of numerical relativity. In: *Astrophys. J* 653 (2006), S. L93–L96. – gr-qc/0603204

[43] Baker, J. G. ; McWilliams, S. T. ; Meter, J. R. ; Centrella, J. ; Choi, D.-I. ; Kelly, B. J. ; Moppitz, M.: Binary black hole late inspiral: Simulations for gravitational wave observations. In: *Phys. Rev.* D75 (2007), S. 124024. – gr-qc/0612117

[44] Baker, J. G. ; Meter, J. R. ; McWilliams, S. T. ; Centrella, J. ; Kelly, B. J.: Consistency of post-Newtonian waveforms with numerical relativity. In: *Phys. Rev. Lett.* 99 (2007), S. 181101. – gr-qc/0612024

[45] Baker *et al.*, J. G.: Modeling kicks from the merger of generic black-hole binaries. In: *Astrophys. J.* 682 (2008), S. L29. – arXiv:0802.0416 [astro-ph]

[46] Balakrishna, J. ; Daues, G. ; Seidel, E. ; Suen, W.-M. ; Tobias, M. ; Wang, E.: Coordinate conditions in three-dimensional numerical relativity. In: *Class. Quantum Grav.* 13 (1996), S. L135–142

[47] Baumgarte, T. ; Brady, P. ; Creighton, J. D. E. ; Lehner, L. ; Pretorius, F. ; De Voe, R.: Learning about compact binary merger: The interplay between numerical relativity and gravitational-wave astronomy. In: *Phys. Rev. D* 77 (2006), S. 084009. – gr-qc/0612100

[48] Baumgarte, T. W.: Innermost stable circular orbit of binary black holes. In: *Phys. Rev. D* 62 (2000), S. 024018. – gr-qc/0004050

[49] Baumgarte, T. W. ; Cook, G. B. ; Scheel, M. A. ; Shapiro, S. L. ; Teukolsky, S. A.: Implementing an apparent-horizon finder in three dimensions. In: *Phys. Rev. D* 54 (1996), S. 4849

[50] Baumgarte, T. W. ; Naculich, S. G.: Analytical Representation of a Black Hole Puncture Solution. In: *Phys. Rev. D* 75 (2007), S. 067502. – gr-qc/0701037

[51] Baumgarte, T. W. ; Shapiro, S. L.: On the Numerical integration of Einstein's field equations. In: *Phys. Rev. D* 59 (1998), S. 024007. – gr-qc/9810065

[52] Baumgarte, T. W. ; Shapiro, S. L.: Numerical relativity and compact binaries. In: *Phys. Rept.* 376 (2003), S. 41–131. – gr-qc/0211028

[53] Beauville, F. ; *et al*: A comparison of methods for gravitational wave burst searches from LIGO and Virgo. In: *Class. Quantum Grav.* 25 (2007), S. 045002. – gr-qc/0701026

[54] Beetle, C. ; Bruni, M. ; Burko, L. M. ; Nerozzi, A.: Towards a novel wave-extraction method for numerical relativity. I. Foundations and initial-value formulation. In: *Phys. Rev. D* 72 (2005), S. 024013

[55] Bekenstein, J. D.: Gravitational-Radiation Recoil and Runaway Black Holes. In: *Astrophys. J.* 183 (1973), S. 657–664

[56] Berger, M. J. ; Oliger, J.: Adaptive Mesh Refinement for Hyperbolic Partial Differential Equations. In: *J. Comput. Phys.* 53 (1984), S. 484–512

[57] Berti, E. ; Cardoso, V.: Quasinormal ringing of Kerr black holes. I: The excitation factors. In: *Phys. Rev. D* 74 (2006), S. 104020. – gr-qc/0605118

[58] Berti, E. ; Cardoso, V. ; González, J. A. ; Sperhake, U. ; Brügmann, B.: Multipolar analysis of spinning binaries. In: *Class. Quantum Grav.* 25 (2008), S. 114035. – arXiv:0711.1097 [gr-qc]

[59] Berti, E. ; Cardoso, V. ; González, J. A. ; Sperhake, U. ; Hannam, M. D. ; Husa, S. ; Brügmann, B.: Inspiral, merger and ringdown of unequal mass black hole binaries: a multipolar analysis. In: *Phys. Rev. D* 76 (2007), S. 064034. – gr-qc/0703053

[60] Blanchet, L.: Innermost circular orbit of binary black holes at the third post-Newtonian approximation. In: *Phys. Rev. D* 65 (2002), S. 124009. – gr-qc/0112056

[61] Blanchet, L.: Gravitational Radiation from Post-Newtonian Sources and Inspiralling Compact Binaries. In: *Living Reviews in Relativity* 9 (2006), Nr. 4. – http://www.livingreviews.org/lrr-2006-4

[62] Blanchet, L. ; Qusailah, M. S. S. ; Will, C. M.: Gravitational recoil of inspiralling black hole binaries to second post-Newtonian order. In: *Astrophys. J* 635 (2005), S. 508–515. – astro-ph/0507692

[63] Bode, T. ; Shoemaker, D. ; Herrmann, F. ; Hinder, I.: Delicacy of Binary Black Hole Mergers in the Presence of Spurious Radiation. In: *Phys. Rev. D* 77 (2008), S. 044027. – arXiv:0711.0669 [gr-qc]

[64] Bogdanović, T. ; Reynolds, C. S. ; Miller, M. C.: Alignment of the spins of supermassive black holes prior to coalescence. In: *Astrophys. J.* 661 (2007), S. L147–L150. – astro-ph/0703054

[65] Bona, C. ; Ledvinka, T. ; Palenzuela, C.: 3+1 covariant suite of numerical relativity evolution systems. In: *Phys. Rev. D* 66 (2002), S. 084013

[66] Bona, C. ; Massó, J.: Hyperbolic evolution systems for numerical relativity. In: *Phys. Rev. Lett.* 68 (1992), S. 1097–1099

[67] Bona, C. ; Massó, J. ; Seidel, E. ; Stela, J.: A New Formalism for Numerical Relativity. In: *Phys. Rev. Lett.* 75 (1995), S. 600–603. – gr-qc/9412071

[68] Bona, C. ; Massó, J. ; Seidel, E. ; Stela, J.: First order hyperbolic formalism for numerical relativity. In: *Phys. Rev. D* 56 (1997), S. 3405–3415. – gr-qc/9709016

[69] Bondi, H. ; Burg, M. G. J. d. ; Metzner, A. W. K.: Gravitational waves in general relativity VII. Waves from axi-symmetric isolated systems. In: *Proc. Roy. Soc. A* 269 (1962), S. 21–52

[70] Bonning, E. ; Marronetti, P. ; Neilsen, D. ; Matzner, R. A.: Physics and initial data for multiple black hole spacetimes. In: *Phys. Rev. D* 68 (2003), S. 044019. – gr-qc/0305071

[71] Bonning, E. W. ; Shields, G. A. ; Salviander, S.: Recoiling Black Holes in Quasars. (2007). – arXiv:0705.4263 [astro-ph]

[72] Bonnor, W. B. ; Rotenberg, M. A.: Transport of momentum by gravitational waves: the linear approximation. In: *Proc. R. Soc. Lond. A.* 265 (1961), S. 109–116

[73] Booth, I.: Black hole boundaries. In: *Can. J. Phys.* 83 (2005), S. 1073–1099. – gr-qc/0508107

[74] Bowen, J. M. ; York, J. W. Jr.: Time-asymmetric initial data for black holes and black-hole collisions. In: *Phys. Rev. D* 21 (1980), S. 2047–2056

[75] Boylan-Kolchin, M. ; Ma, C.-P. ; Quataert, E.: Core Formation in Galactic Nuclei due to Recoiling Black Holes. In: *Astrophys. J* 613 (2004), S. L37–L40. – astro-ph/0407488

[76] Boyle, L. ; Kesden, M.: The spin expansion for binary black hole merger: new predictions and future directions. In: *Phys. Rev. D* 78 (2008), S. 024017. – arXiv:0712.2819 [astro-ph]

[77] Boyle, L. ; Kesden, M. ; Nissanke, S.: Binary black hole merger: symmetry and the spin expansion. In: *Phys. Rev. Lett.* 100 (2008), S. 151101. – arXiv:0709.0299 [gr-qc]

[78] Boyle, M. ; Brown, D. A. ; Kidder, L. E. ; Mroué, A. H. ; Pfeiffer, H. P. ; Scheel, M. A. ; Cook, G. B. ; Teukolsky, S. A.: High-accuracy comparison of numerical relativity simulations with post-Newtonian expansions. In: *Phys. Rev. D* 76 (2007), S. 124038. – arXiv:0710.0158 [gr-qc]

[79] Brandt, S. ; Brügmann, B.: A Simple Construction of Initial Data for Multiple Black Holes. In: *Phys. Rev. Lett.* 78 (1997), S. 3606–3609

[80] Brandt, S. ; Correll, R. ; Gómez, R. ; Huq, M. ; Laguna, P. ; Lehner, L. ; Marronetti, P. ; Matzner, R. A. ; Neilsen, D. ; Pullin, J. ; Schnetter, E. ; Shoemaker, D. ; Winicour, J.: Grazing Collisions of Black Holes via the Excision of Singularities. In: *Phys. Rev. Lett.* 85 (2000), S. 5496–5499. – gr-qc/0009047

[81] Brill, D. R. ; Lindquist, R. W.: Interaction Energy in Geometrostatics. In: *Phys. Rev.* 131 (1963), S. 471–476

[82] Brown, J. D.: Puncture Evolution of Schwarzschild Black Holes. (2007). – arXiv:0705.1359 [gr-qc]

[83] Brügmann, B.: Adaptive mesh and geodesically sliced Schwarzschild spacetime in 3+1 dimensions. In: *Phys. Rev. D* 54 (1996), Nr. 12, S. 7361–7372. – gr-qc/9608050

[84] Brügmann, B.: Binary Black Hole Mergers in 3D Numerical Relativity. In: *Int. J. Mod. Phys.* 8 (1999), S. 85–100. – gr-qc/9708035

[85] Brügmann, B. ; González, J. A. ; Hannam, M. D. ; Husa, S. ; Sperhake, U.: Exploring black hole superkicks. In: *Phys. Rev. D* 77 (2008), S. 124047. – arXiv:0707.0135 [gr-qc]

[86] Brügmann, B. ; González, J. A. ; Hannam, M. D. ; Husa, S. ; Sperhake, U. ; Tichy, W.: Calibration of Moving Puncture Simulations. In: *Phys. Rev. D* 77 (2008), S. 024027. – gr-qc/0610128

[87] Brügmann, B. ; Tichy, W. ; Jansen, N.: Numerical simulation of orbiting black holes. In: *Phys. Rev. Lett.* 92 (2004), S. 211101. – gr-qc/0312112

[88] Bruhat, Y.: The Cauchy problem. In: Witten, L. (Hrsg.): *Gravitation: An Introduction to Current Research*, Wiley, New York, 1962

[89] Buonanno, A. ; Chen, Y. ; Valisneri, M.: Detection template families for gravitational waves from the final stages of binary-black-hole inspirals: Nonspinning case. In: *Phys. Rev. D* 67 (2003), S. 024016. – [Erratum-ibid. **74**, 029903 (2006)], gr-qc/0205122

[90] Buonanno, A. ; Cook, G. B. ; Pretorius, F.: Inspiral, merger and ringdown of equal-mass black-hole binaries. In: *Phys. Rev. D* 75 (2007), S. 124018. – gr-qc/0610122

[91] Buonanno, A. ; Damour, T.: Effective one-body aproach to general relativistic two-body dynamics. In: *Phys. Rev. D* 59 (1999), S. 084006

[92] Buonanno, A. ; Kidder, L. E. ; Lehner, L.: Estimating the final spin of a binary black hole coalescence. In: *Phys. Rev. D* 77 (2008), S. 026004. – arXiv:0709.3839 [astro-ph]

[93] Buonanno, A. ; Pan, Y. ; Baker, J. G. ; Centrella, J. ; Kelly, B. J. ; McWilliams, S. T. ; Meter, J. R.: Toward faithful templates for non-spinning binary black holes using the effective-one-body approach. In: *Phys. Rev. D* 76 (2007), S. 104049. – arXiv:0706.3732 [gr-qc]

[94] Calabrese, G. ; Pullin, J. ; Sarbach, O. ; Tiglio, M.: Convergence and stability in numerical relativity. In: *Phys. Rev. D* 66 (2002), S. 041501

[95] Calabrese, G. ; Pullin, J. ; Sarbach, O. ; Tiglio, M. ; Reula, O.: Well posed constraint-preserving boundary conditions for the linearized Einstein equations. In: *Commun. Math. Phys.* 240 (2003), S. 377–395. – gr-qc/0209017

[96] Campanelli, M: Understanding the fate of merging supermassive black holes. In: *Class. Quantum Grav.* 22 (2005), S. S387–S393. – astro-ph/0411744

[97] Campanelli, M. ; Lousto, C. O.: Second order gauge invariant gravitational perturbations of a Kerr black hole. In: *Phys. Rev. D* 59 (1999), S. 124022. – gr-qc/9811019

[98] Campanelli, M. ; Lousto, C. O. ; Marronetti, P. ; Zlochower, Y.: Accurate Evolutions of Orbiting Black-Hole Binaries without Excision. In: *Phys. Rev. Lett.* 96 (2006), S. 111101. – gr-qc/0511048

[99] Campanelli, M. ; Lousto, C. O. ; Zlochower, Y.: Gravitational radiation from spinning-black-hole binaries: The orbital hang up. In: *Phys. Rev. D* 74 (2006), S. 041501. – gr-qc/0604012

[100] Campanelli, M. ; Lousto, C. O. ; Zlochower, Y.: Last orbit of binary black holes. In: *Phys. Rev. D* 73 (2006), S. 061501(R). – gr-qc/0601091

[101] Campanelli, M. ; Lousto, C. O. ; Zlochower, Y.: Spin-orbit interactions in black-hole binaries. In: *Phys. Rev. D* 74 (2006), S. 084023. – gr-qc/0608275

[102] Campanelli, M. ; Lousto, C. O. ; Zlochower, Y. ; Krishnan, B. ; Merritt, D.: Spin Flips and Precession in Black-Hole-Binary Mergers. In: *Phys. Rev. D* 75 (2007), S. 064030. – gr-qc/0612076

[103] Campanelli, M. ; Lousto, C. O. ; Zlochower, Y. ; Merritt, D.: Large Merger Recoils and Spin Flips From Generic Black-Hole Binaries. In: *Astrophys. J.* 659 (2007), S. L5–L8. – gr-qc/0701164

[104] Campanelli, M. ; Lousto, C. O. ; Zlochower, Y. ; Merritt, D.: Maximum gravitational recoil. In: *Phys. Rev. Lett.* 98 (2007), S. 231102. – gr-qc/0702133

[105] Chandrasekhar, S. ; Detweiler, S.: The quasi-normal modes of the Schwarzschild black hole. In: *Proc. R. Soc. Lond. A.* 344 (1975), S. 441–452

[106] Choi, D.-I. ; Kelly, B. J. ; Boggs, W. D. ; Baker, J. G. ; Centrella, J. ; Meter, J. van: Recoiling from a kick in the head-on collision of spinning black holes. In: *Phys. Rev. D* 76 (2007), S. 104026. – gr-qc/0702016

[107] Choptuik, M. W.: Universality and Scaling in Graviational Collapse of a Massless Scalar Field. In: *Phys. Rev. Lett.* 70 (1993), S. 9–12

[108] Christodoulou, D: Reversible and Irreversible Transformations in Black Hole Physics. In: *Phys. Rev. Lett.* 25 (1970), S. 1596–1597

[109] Cook, G. B.: Three-dimensional initial data for the collision of two black holes. II. Quasicircular orbits for equal-mass black holes. In: *Phys. Rev. D* 50 (1994), S. 5025–5032. – gr-qc/9404043

[110] Cook, G. B.: Initial Data for Numerical Relativity. In: *Living Reviews in Relativity* 2000-5 (2000). – [Online Article] cited on 30 Sep 2004, http://relativity.livingreviews.org/Articles/lrr-2000-5

[111] Cook, G. B.: Corotating and irrotational binary black holes in quasicircular orbits. In: *Phys. Rev. D* 65 (2002), S. 084003

[112] Cook, G. B. ; Pfeiffer, H.: Excision boundary conditions for black hole initial data. In: *Phys. Rev. D* 70 (2004), S. 104016. – gr-qc/0407078

[113] Cook *et al.*, G. B.: Boosted three-dimensional black-hole evolutions with singularity excision. In: *Phys. Rev. lett.* 80 (1998), S. 2512–2516. – gr-qc/9711078

[114] Dain, S. ; Jaramillo, J. L. ; Krishnan, B.: On the existence of initial data containing isolated black holes. In: *Phys. Rev. D* 71 (2004), S. 064003. – gr-qc/0412061

[115] Damour, T. ; Gopakumar, A.: Gravitational recoil during binary black hole coalescence using the effective one body approach. In: *Phys. Rev. D* 73 (2006), S. 124006. – gr-qc/0602117

[116] Damour, T. ; Gourgoulhon, E. ; Grandclément, P.: Circular orbits of corotating binary black holes: Comparison between analytical and numerical results. In: *Phys. Rev. D* 66 (2002), S. 024007. – gr-qc/0204011

[117] Damour, T. ; Jaranowski, P. ; Schäfer, G.: Determination of the last stable orbit for circular general relativistic binaries at the third post-Newtonian approximation. In: *Phys. Rev. D* 62 (2000), S. 084011

[118] Damour, T. ; Jaranowski, P. ; Schäfer, G.: Dynamical invariants for general relativistic two-body systems at the third post-Newtonian approximation. In: *Phys. Rev. D* 62 (2000), S. 044024. – gr-qc/9912092

[119] Damour, T. ; Nagar, A.: Final spin of a coalescing black-hole binary: An effective-one-body approach. In: *Phys. Rev. D* 76 (2007), S. 044003. – arXiv:0704.3550 [gr-qc]

[120] Damour, T. ; Nagar, A.: Comparing Effective-One-Body gravitational waveforms to accurate numerical data. In: *Phys. Rev. D* 77 (2008), S. 024043. – arXiv:0711.2628 [gr-qc]

[121] Damour, T. ; Nagar, A. ; Dorband, E. N. ; Pollney, D. ; Rezzolla, L.: Faithful Effctive-One-Body waveforms of equal-mass coalescing black-hole binaries. In: *Phys. Rev. D* 77 (2008), S. 084017. – arXiv:0712.3003 [gr-qc]

[122] Damour, T. ; Nagar, A. ; Hannam, M. D. ; Husa, S. ; Brügmann, B.: Accurate Effective-One-Body waveforms of inspiralling and coalescing black-hole binaries. In: *Phys. Rev. D* 78 (2008), S. 044039. – arXiv:[0803.3162]

[123] Diener, P. ; Herrmann, F. ; Pollney, D. ; Schnetter, E. ; Seidel, E. ; Takahashi, R. ; Thornburg, J. ; Ventrella, J.: Accurate Evolution of Orbiting Binary Black Holes. In: *Phys. Rev. Lett.* 96 (2006), S. 121101. – gr-qc/0512108

[124] Dreyer, O. ; Krishnan, B. ; Schnetter, E. ; Shoemaker, D.: Introduction to Isolated Horizons in Numerical Relativity. In: *Phys. Rev. D* 67 (2003), S. 024018. – gr-qc/0206008

[125] Drown, D. A. ; Babak, S. ; Brady, P. R. ; Christensen, N. ; Cokelaer, T. ; Creighton, J. D. E. ; Fairhurst, S. ; González, G. ; Messaritaki, E. ; Sathyaprakash, B. S. ; Shawhan, P. ; Zotov, N.: Searching for gravitational waves from binary inspiral with LIGO. In: *Class. Quantum Grav.* 21 (2004), S. S1625–S1633

[126] Efstathiou, G. ; Rees, M.: High-redshift quasars in the Cold Dark Matter cosmogony. In: *MNRAS* 230 (1988), S. 5

[127] Eppley, K. R.: *The numerical evolution of the collision of two black holes*, Princeton University, Diss., 1975

[128] Etienne, Z. B. ; Faber, J. A. ; Liu, Y. T. ; Shapiro, S. L. ; Taniguchi, K. ; Baumgarte, T. W.: Fully General Relativistic Simulations of Black-Hole-Neutron Star Mergers. In: *Phys. Rev. D* 77 (2008), S. 084002. – arXiv:0712.2460 [astro-ph]

[129] Fan, X. ; Strauss, M. A. ; Schneider, D. P. ; Becker, R. H. ; White, R. L. ; Haiman, Z. ; Gregg, M. ; Pentericci, L. ; Grebel, E. K. ; Narayanan, V. K. ; Loh, Y.-S. ; Richards, G. T. ; Gunn, J. E. ; Lupton, R. H. ; Knapp, G. R. ; Ivezić, Z. ; Brandt, W. N. ; Collinge, M. ; Hao, L. ; Harbeck, D. ; Prada, F. ; Schaye, J. ; Strateva, I. ; Zakamska, N. ; Anderson, S. ; Brinkmann, J. ; Bahcall, N. A. ; Lamb, D. Q. ; Okamura, S. ; Szalay, A. ; York, D. G.: A Survey of z¿5.7 Quasars in the Sloan Digital Sky Survey. II. Discovery of Three Additional Quasars at z¿6. In: *Astron. J* 125 (2003), S. 1649–1659. – astro-ph/0301135

[130] Favata, M. ; Hughes, S. A. ; Holz, D. E.: How black holes get their kicks: Gravitational radiation recoil revisited. In: *Astrophys. J* 607 (2004), S. L5–8. – astro-ph/0408492

[131] Ferrares, L. ; Merritt, D.: A Fundamental Relation between Supermassive Black Holes and Their Host Galaxies. In: *Astrophys. J* 539 (2000), S. L9–L12. – astro-ph/0006053

[132] Ferrarese, L. ; Ford, H.: Supermassive Black Holes in Galactic Nuclei: Past, Present and Future Research. In: *Sp. Sci. Rev.* 116, S. 523. – astro-ph/0411247

[133] Fiske, D. R. ; Baker, J. G. ; Meter, J. R. ; Choi, D.-I. ; Centrella, J. M.: Wave zone extraction of gravitational radiation in three-dimensional numerical relativity. In: *Phys. Rev. D* 71 (2005), S. 104036. – gr-qc/0503100

[134] Fitchett, M. J.: The influence of gravitational wave momentum losses on the centre of mass motion of a Newtonian binary system. In: *MNRAS* 203 (1983), S. 1049–1062

[135] Fitchett, M. J. ; Detweiler, S.: Linear momentum and gravitational waves - Circular orbits around a Schwarzschild black hole. In: *MNRAS* 211 (1984), S. 933

[136] Frauendiener, J.: Conformal Infinity. In: *Living Reviews in Relativity* 2004-1 (2004). – [Article in Online Journal] cited on 19 Feb 2008, http://relativity.livingreviews.org/Articles/lrr-2004-1/download/index.html

[137] Friedrich, H.: Cauchy problems for the conformal vacuum field equations in General Relativity. In: *Comm. Math. Phys.* 91 (1983), S. 445

[138] Friedrich, H.: On the Hyperbolicity of Einstein's and Other Gauge Field Equations. In: *Comm. Math. Phys.* 100 (1985), S. 525

[139] Friedrich, H.: Hyperbolic reductions for Einstein's equations. In: *Class. Quantum Grav.* 13 (1996), S. 1451–1469

[140] Friedrich, H. ; Nagy, G.: The initial boundary value problem for Einstein's vacuum field equations. In: *Commun. Math. Phys.* 201 (1999), S. 619

[141] Frittelli, S. ; Gomez, R.: Einstein boundary conditions in relation to constraint propagation for the initial-boundary value problem of the Einstein equations. In: *Phys. Rev. D* 69 (2004), S. 124020. – gr-qc/0310064

[142] Frittelli, S. ; Reula, O. A.: First-Order Symmetric Hyperbolic Einstein Equations with Arbitrary Fixed Gauge. In: *Phys. Rev. Lett.* 76 (1996), S. 4667–4670. – gr-qc/9605005

[143] Garat, A. ; Price, R. H.: Nonexistence of conformally flat slices of the Kerr spacetime. In: *Phys. Rev. D* 61 (2000), S. 124011. – gr-qc/0002013

[144] Garfinkle, D.: Harmonic coordinate method for simulating generic singularities. In: *Phys. Rev. D* 65 (2002), S. 044029. – gr-qc/0110013

[145] Gebhardt, K. ; Bender, R. ; Bower, G. ; Dressler, A. ; Faber, S. M. ; Filippenko, A. V. ; Green, R. ; Grillmair, C. ; Ho, L. C. ; Kormendy, J. ; Lauer, T. R. ; Magorrian, J. ; Pinkney, J. ; Richstone, S. D. T. D. Tremaine: A Relationship between Nuclear Black Hole Mass and Galaxy Velocity Dispersion. In: *Astrophys. J* 539 (2000), S. L13–L19. – astro-ph/0006289

[146] González, J. A. ; Hannam, M. D. ; Sperhake, U. ; Brügmann, B. ; Husa, S.: Supermassive kicks for spinning black holes. In: *Phys. Rev. Lett.* 98 (2007), S. 231101. – gr-qc/0702052

[147] González, J. A. ; Sperhake, U. ; Brügmann, B. ; Hannam, M. D. ; Husa, S.: The maximum kick from nonspinning black-hole binary inspiral. In: *Phys. Rev. Lett.* 98 (2007), S. 091101. – gr-qc/0610154

[148] Gourgoulhon, E.: *3+1 Formalism and Bases of Numerical Relativity.* – gr-qc/0703035

[149] Gourgoulhon, E. ; Grandcl ement, P. ; Bonazzola, S.: Binary black holes in circular orbits. I. A global spacetime approach. In: *Phys. Rev. D* 65 (2002), S. 044020. – gr-qc/0106015

[150] Gourgoulhon, E. ; Jaramillo, J. L.: A 3+1 perspective on null hypersurfaces and isolated horizons. In: *Phys. Rept.* 423 (2006), S. 159. – gr-qc/0503113

[151] Grandclément, P. ; Gourgoulhon, E. ; Bonazzola, S.: Binary black holes in circular orbits. II. Numerical methods and first results. In: *Phys. Rev. D* 65 (2002), S. 044021. – gr-qc/0106016

[152] Grandclement, P. ; Novak, J.: Spectral Methods for Numerical Relativity. (2007). – arXiv:0706.2286 [gr-qc]

[153] Gualandris, A. ; Merritt, D.: Ejection of Supermassive Black Holes from Galaxy Cores. In: *Astrophys. J* 678 (2008), S. 780–797. – arXiv:0708.0771 [astro-ph]

[154] Gundlach, C. ; Calabrese, G. ; Hinder, I. ; Martín-García, J. M.: Constraint damping in the Z4 formulation and harmonic gauge. In: *Class. Quantum Grav.* 22 (2005), S. 3767–3773

[155] Gundlach, C. ; Martín-García, J. M.: Symmetric hyperbolic form of systems of second-order evolution equations subject to constraints. In: *Phys. Rev. D* 70 (2004), S. 044031. – gr-qc/0403019

[156] Gundlach, C. ; Martín-García, J. M.: Symmetric hyperbolicity and consistent boundary conditions for second-order Einstein equations. In: *Phys. Rev. D* 70 (2004), S. 044032. – gr-qc/0403019

[157] Haehnelt, M. G. ; Davies, M. B. ; Rees, M. J.: Possible evidence for the ejection of a supermassive black hole from an ongoing merger of galaxies. In: *MNRAS* 366 (2005), S. L22–L25

[158] Hahn, S. G. ; Lindquist, R. W.: The two body problem in geometrodynamics. In: *Ann. Phys.* 29 (1964), S. 304–331

[159] Haiman, Z.: Constraints from Gravitational Recoil on the Growth of Supermassive Black Holes at High Redshift. In: *Astrophys. J* 613 (2004), S. 36–40. – astro-ph/0404196

[160] Haiman, Z. ; Loeb, A.: What is the highest plausible redshift of luminous quasars? In: *Astrophys. J.* 552 (2001), S. 459–463

[161] Hannam, M. ; Husa, S. ; Ó Murchadha, N. ; Brügmann, B. ; González, J. A. ; Sperhake, U.: Where do moving punctures go? In: *J. Phys. Conf. Ser.* 66 (2007), S. 012047. – gr-qc/0612097

[162] Hannam, M. ; Husa, S. ; Ohme, F. ; Brügmann, B. ; Ó Murchadha, N.: Wormholes and trumpets: the Schwarzschild spacetime for the moving-puncture generation. (2008). – 0804.0628

[163] Hannam, M. D. ; Husa, S. ; Brügmann, B. ; Gopakumar, A.: Comparison between numerical-relativity and post-Newtonian waveforms from spinning binaries: the orbital hang-up case. In: *Phys. Rev. D* 78 (2008), S. 104007. – arXiv:0712.3787 [gr-qc]

[164] Hannam, M. D. ; Husa, S. ; González, J. A. ; Sperhake, U. ; Brügmann, B.: Where post-Newtonian and numerical-relativity waveforms meet. In: *Phys. Rev. D* 77 (2008), S. 044020. – arXiv:0706.1305 [gr-qc]

[165] Hannam, M. D. ; Husa, S. ; Pollney, D. ; Brügmann, B. ; Ó Murchadha, N.: Geometry and Regularity of Moving Punctures. In: *Phys. Rev. Lett.* 99 (2007), S. 241102. – gr-qc/0606099

[166] Hawking, S. W. ; Ellis, G. F. R.: *The Large Scale Structure of Space-Time.* Cambridge University Press, 1973

[167] Hawking, S. W. ; Penrose, R.: The singularities of gravitational collapse and cosmology. In: *Proc. Roy. Soc. Lond.* 314 (1970), S. 529

[168] Heinzel *et al.*, G.: LISA interferometry: recent developments. In: *Class. Quantum Grav.* 23 (2006), S. S119–S124

[169] Herrmann, F. ; Hinder, I. ; Shoemaker, D. ; Laguna, P.: Unequal-Mass Binary Black Hole Plunges and Gravitational Recoil. In: *Class. Quantum Grav.* 24 (2007), S. S33–S42. – gr-qc/0601026

[170] Herrmann, F. ; Hinder, I. ; Shoemaker, D. ; Laguna, P. ; Matzner, R. A.: Gravitational recoil from spinning binary black hole mergers. In: *Astrophys. J.* 661 (2007), S. 430. – gr-qc/0701143

[171] Herrmann, F. ; Hinder, I. ; Shoemaker, D. M. ; Laguna, P. ; Matzner, R. A.: Binary Black Holes: Spin Dynamics and Gravitational Recoil. In: *Phys. Rev. D* 76 (2007), S. 084032. – arXiv:0706.2541

[172] Hinder, I. ; Vaishnav, B. ; Herrmann, F. ; Shoemaker, D. ; Laguna, P.: Circularization and Final Spin in Eccentric Binary Black Hole Inspirals. In: *Phys. Rev. D* 77 (2008), S. 081502. – arXiv:0710.5167 [gr-qc]

[173] Hoffman, L. ; Loeb, A.: Three-body kick to a bright quasar out of its galaxy during a merger. In: *Astrophys. J.* 638 (2006), S. L75–L78

[174] Holley-Bockelmann, K. ; Gultekin, K. ; Shoemaker, D. ; Yunes, N.: Gravitational Wave Recoil and the Retention of Intermediate Mass Black Holes. (2007). – arXiv:0707.1334 [astro-ph]

[175] Hughes, S. A.: (Sort of) Testing relativity with extreme mass ratio inspirals. In: *AIP Conf. Proc.* 873 (2006), S. 233–240. – gr-qc/0608140

[176] Hughes, S. A.: LISA sources and science. (2007). – arXiv:0711.0188 [gr-qc]

[177] Hulse, R. A. ; Taylor, J. H.: Discovery of a Pulsar in a Binary System. In: *Astrophys. J.* 195 (1975), S. L51–55

[178] Huq, M. F. ; Choptuik, M. W. ; Matzner, R. A.: Locating boosted Kerr and Schwarzschild apparent horizons. In: *Phys. Rev. D* 66 (2002), S. 084024

[179] Husa, S. ; González, J. A. ; Hannam, M. D. ; Brügmann, B. ; Sperhake, U.: Reducing phase error in long numerical binary black hole evolutions with sixth order finite differencing. In: *Class. Quant. Grav.* 25 (2008), S. 105006. – arXiv:0706.0740 [gr-qc]

[180] Husa, S. ; Hannam, M. ; González, J. A. ; Sperhake, U. ; Brügmann, B.: Reducing eccentricity in black-hole binary evolutions with initial parameters from post-Newtonian inspiral. In: *Phys. Rev.D* 77 (2008), S. 044037. – arXiv:0706.0904 [gr-qc]

[181] Jaramillo, J. L. ; Gourgoulhon, E. ; Mena Marugan, G. A.: Inner boundary conditions for black hole Initial Data derived from Isolated Horizons. In: *Phys. Rev. D* 70 (2004), S. 124036. – gr-qc/0407063

[182] Jaramillo, J. L. ; Valiente Kroon, J. A. ; Gourgoulhon, E.: From Geometry to Numerics: interdisciplinary aspects in mathematical and numerical relativity. (2007). – arXiv:0712.2332 [gr-qc]

[183] Kerr, R. P.: Gravitational Field of a Spinning Mass as an Example of Algebraically Special Metrics. In: *Phys. Rev. Lett.* 11 (1963), S. 237–238

[184] Kerr, R. P. ; Schild, A.: Some algebraically degenerate solutions of Einstein's gravitational field equations. In: *Proceedings of Symposia in Applied Mathematics Vol XVII*, 1965, S. 199–209

[185] Khokhlov, A. M. ; Novikov, I. D.: Gauge stability of 3 + 1 formulations of general relativity. In: *Class. Quantum Grav.* 19 (2002), S. 827–846

[186] Kidder, L. E.: Coalescing binary systems of compact onjects to (post)^5/2-Newtonian order. V. Spin effects. In: *Phys. Rev. D* 52 (1995), S. 821–847

[187] Kidder, L. E. ; Lindblom, L. ; Scheel, M. A. ; Buchman, L. T. ; Pfeiffer, H. P.: Boundary conditions for the Einstein evolution system. In: *Phys. Rev. D* 71 (2005), S. 064020. – gr-qc/0412116

[188] Kidder, L. E. ; Scheel, M. A. ; Teukolsky, S. A.: Extending the lifetime of 3D black hole computations with a new hyperbolic system of evolution equations. In: *Phys. Rev. D* 64 (2001), S. 064017. – gr-qc/0105031

[189] Kidder, L. E. ; Will, C. M. ; Wiseman, A. G.: Innermost stable orbits for coalescing binary systems of compact objects. In: *Class. Quantum Grav.* 9 (1992), S. L125–L131

[190] Kinnersley, W.: Type D Vacuum Metrics. In: *J. Math. Phys.* 10 (1969), S. 1195–1203

[191] Kokkotas, K. ; Schmidt, B. G.: Quasi-Normal Modes of Stars and Black Holes. In: *Living Reviews in Relativity* 2 (1999), Nr. 2. – http://www.livingreviews.org/lrr-1999-2

[192] Koppitz, M. ; Pollney, D. ; Reisswig, C. ; Rezzolla, L. ; Thornburg, J. ; Diener, P. ; Schnetter, E.: Recoil Velocities from Equal-Mass Binary-Black-Hole Mergers. In: *Phys. Rev. Lett.* 99 (2007), S. 041102. – gr-qc/0701163

[193] Kormendy, J. ; Richstone, D.: Inward bound – The search for supermassive black holes in galactic nuclei. In: *ARA&A* 33 (1995), S. 581–624

[194] Krishnan, B.: Fundamental properties and applications of quasi-local black hole horizons. (2007). – arXiv:0712.1575 [gr-qc]

[195] Laguna, P. ; Shoemaker, D.: Numerical stability of a new conformal-traceless 3+1 formulation of the Einstein equation. In: *Class. Quantum Grav.* 19 (2002), S. 3679–3686

[196] Leahy, J. P. ; Parma, P.: Multiple outbursts in radio galaxies. In: Roland, J. (Hrsg.) ; Sol, H. (Hrsg.) ; Pelletier, G. (Hrsg.): *7.IAP Meeting: Extragalactic radio sources - from beams to jets*, 1992, S. 307–308

[197] Leaver, E. W.: Spectral decomposition of the perturbation response of the Schwarzschild geometry. In: *Phys. Rev. D* 34 (1986), S. 384–408

[198] Lehner, L.: Numerical Relatvity: A review. In: *Class. Quant. Grav.* 18 (2001), S. R25–R86. – gr-qc/0106072

[199] Lehner, L. ; Moreschi, O. M.: Dealing with delicate issues in waveform calculations. In: *Phys. Rev. D* 76 (2007), S. 124040. – arXiv:0706.1319 [gr-qc]

[200] Libeskind, N. I. ; Cole, S. ; Frenk, C. S. ; Helly, J. C.: The effect of gravitational recoil on black holes forming in a hierarchical universe. In: *MNRAS* 368 (2006), S. 1381–1391. – astro-ph/0512073

[201] Lichnerowicz, A.: L'integration des équations de la gravitation relativiste et le problème des n corps. In: *J. Math. Pures et Appl.* 23 (1944), S. 37–63

[202] Liebling, S.: Singularity threshold of the nonlinear sigma model using 3D adaptive mesh refinement. In: *Phys. Rev. D* 66 (2002), S. 041703(R)

[203] Lindblom, L. ; Scheel, M. A. ; Kidder, L. E. ; Owen, R. ; Rinne, O.: A New Generalized Harmonic Evolution System. In: *Class. Quant. Grav.* 23 (2006), S. S447–S462. – gr-qc/0512093

[204] Lippai, Z. ; Frei, Z. ; Haiman, Z.: Prompt Shocks in the Gas Disk Around a Recoiling Supermassive Black Hole Binary. (2008). – arXiv:0801.0739 [astro-ph]

[205] Loeb, A.: Observable Signatures of a Black Hole Ejected by Gravitational Radiation Recoil in a Galaxy Merger. In: *Phys. Rev. Lett.* 99 (2007), S. 041103. – astro-ph/0703722

[206] Lousto, Carlos O. ; Zlochower, Yosef: Further insight into gravitational recoil. In: *Phys. Rev. D* 77 (2008), S. 044028. – arXiv:0708.4048 [gr-qc]

[207] Lueck *et al.*, H.: Status of the GEO600 detector. In: *Class. Quantum Grav.* 23 (2006), S. S71–S78

[208] MacNeice, P. ; Olson, K. ; Mobarry, C. ; Fainchtein, R. de ; Packer, C.: PARAMESH: A Parallel Adaptive Mesh Refinement Community Toolkit. In: *Computer Physics Comm.* 136 (2000), S. 330

[209] Madau, P. ; Quataert, E.: The effect of gravitational-wave recoil on the demography of massive black holes. In: *Astrophys. J.* 606 (2004), S. L17–L20

[210] Madau, P. ; Rees, M. J. ; Volonteri, M. ; Haardt, F. ; Oh, S. P.: Early reionization by miniquasars. In: *Astrophys. J.* 604 (2004), S. 484–494

[211] Magain, P. ; Letawe, G. ; Courbin, F. ; Jablonka, P. ; Jahnke, K. ; Meylan, G. ; Wisotzki, L.: Discovery of a bright quasar without a massive host galaxy. In: *Nature* 437 (2005), S. 381–384

[212] Marronetti, P. ; Duez, M. D. ; Shapiro, S. L. ; Baumgarte, T.: Dynamical Determination of the Innermost Stable Circular Orbit of Binary Neutron Stars. In: *Phys. Rev. Lett.* 92 (2004), S. 141101. – gr-qc/0312036

[213] Marronetti, P. ; Huq, M. ; Laguna, P. ; Lehner, L. ; Matzner, R. ; Shoemaker, D.: Approximate analytical solutions to the initial data problem of black hole binary systems. In: *Phys. Rev. D* 62 (2000), S. 024017. – gr-qc/0001077

[214] Marronetti, P. ; Matzner, R. A.: Solving the Initial Value Problem of two Black Holes. In: *Phys. Rev. Lett.* 85 (2000), S. 5500–5503

[215] Marronetti, P. ; Tichy, W. ; Brügmann, B. ; González, J. A. ; Sperhake, U.: High-spinning binary black hole mergers. In: *Phys. Rev. D* 77 (2008), S. 064010. – arXiv:0709.2160 [gr-qc]

[216] Matzner, R. A. ; Huq, M. F. ; Shoemaker, D.: Initial data and coordinates for multiple black hole systems. In: *Phys. Rev. D* 59 (1998), S. 024015. – gr-qc/9805023

[217] Merritt, D. ; Ekers, R. D.: Tracing Black Hole Mergers Through Radio Lobe Morphology. In: *Science* 297 (2002), S. 1310–1313

[218] Merritt, D. ; Ferrarese, L.: Black hole demographics from the $M_\bullet$-σ relation. In: *MNRAS* 320 (2001), S. L30–L34. – astro-ph/0009076

[219] Merritt, D. ; Milosavljević, M. ; Favata, M. ; Hughes, S. ; Holz, D.: Consequences of Gravitational Radiation Recoil. In: *Astrophys. J* 607 (2004), S. L9–L12. – astro-ph/0402057

[220] Merritt, D. ; Storchi-Bergmann, T. ; Robinson, D. ; Batcheldor, D. ; Axon, D. ; Fernandes, R. C.: The nature of the HE0450-2958 system. In: *MNRAS* 367 (2006), S. 1746–1750. – astro-ph/0511315

[221] Meter, J. R. ; Baker, J. G. ; Koppitz, M. ; Choi, D.-I.: How to move a black hole without excision: gauge conditions for the numerical evolution of a moving puncture. In: *Phys. Rev.* D73 (2006), S. 124011. – gr-qc/0605030

[222] Miller, M. ; Gressman, P. ; Suen, W.-M.: Towards a realistic neutron star binary inspiral: Initial data and multple orbit evolution in full general relativity. In: *Phys. Rev. D* 69 (2004), S. 064026. – gr-qc/0312030

[223] Milosavljević, M. ; Merrit, D.: Formation of galactic nuclei. In: *Astrophys. J.* 563 (2001), S. 34–62

[224] Misner, C. ; Wheeler, J.: Classical physics as geometry. In: *Ann. Phys. (N.Y.)* 2 (1957), S. 525

[225] Misner, C. W.: Wormhole initial conditions. In: *Phys. Rev.* 118 (1960), S. 1110

[226] Misner, C. W. ; Thorne, K. S. ; Wheeler, J. A.: *Gravitation*. W. H. Freeman, New York, 1973

[227] Moncrief, V.: Gravitational Perturbations of Spherically Symmetric Systems. I. The Exterior Problem. In: *Ann. Phys.* 88 (1974), S. 323–343

[228] Nagy, G. ; Ortiz, O. E. ; Reula, O. A.: Strongly hyperbolic second order Einstein's evolution equations. In: *Phys. Rev. D* 70 (2004), S. 044012

[229] Nerozzi, A.: Scalar functions for wave extraction in numerical relativity. In: *Phys. Rev. D* 75 (2007), S. 104002

[230] Nerozzi, A. ; Beetle, C. ; Bruni, M. ; Burko, L. M. ; Pollney, D.: Towards wave extraction in numerical relativity: the quasi-Kinnersley frame. In: *Phys. Rev. D* 72 (2005), S. 024014

[231] Nerozzi, A. ; Bruni, M. ; Re, V. ; Burko, L. M.: Towards a wave-extraction method for numerical relativity: IV. Testing the quasi-Kinnersley method in the Bondi-Sachs framework. In: *Phys. Rev. D* 73 (2006), S. 044020

[232] Newman, E. T. ; Penrose, R.: An Approach to Gravitational Radiation by a Method of Spin Coefficients. In: *J. Math. Phys.* 3 (1962), S. 566–578

[233] Ó Murchadha, N. ; York, J. W. Jr.: Initial-value problem of general relativity. I. General formulation and interpretation. In: *Phys. Rev. D* 10 (1974), S. 428–436

[234] Ó Murchadha, N. ; York, J. W. Jr.: Initial-value problem of general relativity. II. Stability of solution of the initial-value equations. In: *Phys. Rev. D* 10 (1974), S. 437–446

[235] Ó Murchadha, N. ; York, J. W. Jr.: Gravitational Potentials: A Constructive Approach to General Relativity. In: *Gen. Relativ. Gravit.* 7 (1976), S. 257–261

[236] O'Leary, R. ; O'Shaughnessy, E. ; Rasio, F.: Dynamical Interactions and the Black Hole Merger Rate of the Universe. In: *Phys. Rev. D* 76 (2007), S. 061504. – astro-ph/0701887

[237] Palenzuela, C. ; Lehner, L. ; Liebling, S. L.: Orbital Dynamics of Binary Boson Star Systems. (2007). – arXiv:0706.2435 [gr-qc]

[238] Pan, Y. ; Buonanno, A. ; Baker, J. G. ; Centrella, J. ; Kelly, B. J. ; McWilliams, S. T. ; Pretorius, F. ; Meter, J. R.: A data-analysis driven comparison of analytic and numerical coalescing binary waveforms: nonspinning case. In: *Phys. Rev. D* 77 (2008), S. 024014. – gr-qc/0704.1964

[239] Parman, P. ; Ekers, R. D. ; Fanti, R.: High resolution radio observations of low luminosity radio galaxies. In: *Astron. Astrophys. Suppl. Ser.* 59 (1985), S. 511–521

[240] Peres, A.: Classical Radiation Recoil. In: *Phys. Rev.* 128 (1962), S. 2471–2475

[241] Peters, P. C.: Gravitational Radiation and the Motion of Two Point Masses. In: *Phys. Rev.* 136 (1964), S. B1224–B1232

[242] Pfeiffer, H.: *Initial data for black hole evolutions*, Cornell University, Diss., 2003. – gr-qc/0510016

[243] Pfeiffer, H. P. ; Brown, D. A. ; Kidder, L. E. ; Lindblom, L. ; Lovelace, G. ; Scheel, M.: Reducing orbital eccentricity in binary black hole simulations. In: *Class. Quantum Grav.* 24 (2007), S. S59–S82. – gr-qc/0702106

[244] Pfeiffer, H. P. ; Teukolsky, S. A. ; Cook, G. B.: Quasicircular orbits for spinning binary black holes. In: *Phys. Rev. D* 62 (2000), S. 104018

[245] Poisson, E.: The Motion of Point Particles in Curved Spacetime. In: *Living Reviews in Relativity* 7 (2004), Nr. 6. – http://www.livingreviews.org/lrr-2004-6

[246] Pollney *et al.*, D.: Recoil velocities from equal-mass binary black-hole mergers: a systematic investigation of spin-orbit aligned configurations. In: *Phys. Rev. D* 76 (2007), S. 124002. – arXiv:0707.2559 [gr-qc]

[247] Pretorius, F.: Evolution of Binary Black-Hole Spacetimes. In: *Phys. Rev. Lett.* 95 (2005), S. 121101. – gr-qc/0507014

[248] Pretorius, F.: Numerical relativity using a generalized harmonic decomposition. In: *Class. Quantum Grav.* 22 (2005), S. 425–451. – gr-qc/0407110

[249] Pretorius, F.: Simulation of Binary-Black-Hole Spacetimes with a Harmonic Evolution Scheme. In: *Class. Quantum Grav.* 23 (2006), S. S529–S552. – gr-qc/0602115

[250] Pretorius, F. ; Choptuik, M. W.: Adaptive Mesh Refinement for Coupled Elliptic-Hyperbolic Systems. In: *J. Comput. Phys.* 218 (2006), Nr. 1, S. 246–274. – http://arXiv.org/abs/gr-qc/0508110

[251] Pretorius, F. ; Khurana, D.: Black Hole Mergers and Unstable Circular Orbits. In: *Class. Quantum Grav.* 24 (2007), S. S83–S108. – gr-qc/0702084

[252] Pretorius, Frans: Binary Black Hole Coalescence. In: Colpi *et al.*, M. (Hrsg.): *Physics of Relativistic Objects in Compact Binaries: From Birth to Coalescence*, Springer, New York, 2009. – arXiv:0710.1338 [gr-qc]

[253] Reimann, B. ; Alcubierre, M. ; González, J. A. ; Nuñez, D.: Constraint and gauge shocks in one-dimensional numerical relativity. In: *Phys. Rev. D* 71 (2005), S. 064021. – gr-qc/0411094

[254] Rezzolla, L. ; Barausse, E. ; Dorband, E. N. ; Pollney, D. ; Reisswig, C. ; Seiler, J. ; Husa, S.: Final spin from the coalescence of two black holes. In: *Physical Review D* 78 (2008), S. 044002. – arXiv:0712.3541 [gr-qc]

[255] Rezzolla, L. ; Diener, P. ; Dorband, E. N. ; Pollney, D. ; Reisswig, C. ; Schnetter, E.: The final spin from the coalescence of aligned-spin black-hole binaries. In: *Astrophys. J.* 674 (2008), S. L29–L32. – arXiv:0710.3345 [gr-qc]

[256] Rezzolla, L. ; Dorband, E. N. ; C., Reisswig. ; Diener, P. ; Pollney, D. ; Schnetter, E. ; Szilagyi, B.: Spin Diagrams for Equal-Mass Black-Hole Binaries with Aligned Spins. In: *Astrophys. J.* 679 (2008), S. 1422. – arXiv:0708.3999

[257] Ruiz, M. ; Alcubierre, M. ; Nuñez, D. ; Takahashi, R.: Multipole expansions for energy and momenta carried by gravitational waves. In: *Gen. Rel. Grav.* 40 (2008), S. 2467. – arXiv:0707.4654 [gr-qc]

[258] Sachs, R. K.: Gravitational waves in general relativity. In: *Proc. Roy. Soc. A* 270 (1962), S. 103–126

[259] Sarbach, O. ; Calabrese, G. ; Pullin, J. ; Tiglio, M.: Hyperbolicity of the BSSN system of Einstein evolution equations. In: *Phys. Rev. D* 66 (2002), S. 064002. – gr-qc/0205064

[260] Sarbach, O. ; Tiglio, M.: Exploiting gauge and constraint freedom in hyperbolic formulations of Einstein's equations. In: *Phys. Rev. D* 66 (2002), S. 064023. – gr-qc/0205086

[261] Sarbach, O. ; Tiglio, M.: Boundary conditions for Einstein's field equations: Analytical and numerical analysis. In: *J. Hyperbol. Diff. Equat.* 2 (2005), S. 839. – gr-qc/0412115

[262] Scheel, M. A. ; Pfeiffer, H. P. ; Lindblom, L. ; Kidder, L. E. ; Rinne, O. ; Teukolsky, S. A.: Solving Einstein's Equations With Dual Coordinate Frames. In: *Phys. Rev. D* 74 (2006), S. 104006. – gr-qc/0607056

[263] Schnetter, E. ; Hawley, S. H. ; Hawke, I.: Evolutions in 3D numerical relativity using fixed mesh refinement. In: *Class. Quantum Grav.* 21 (2004), S. 1465–1488. – gr-qc/0310042

[264] Schnittman, J. D. ; Buonanno, A.: The Distribution of Recoil Velocities from Merging Black Holes. In: *Astrophys. J.* 662 (2007), S. L63–L66. – astro-ph/0702641

[265] Schnittman, J. D. ; Buonanno, A. ; Meter, J. R. ; Baker, J. G. ; Boggs, W. D. ; Centrella, J. ; Kelly, B. J. ; McWilliams, S. T.: Anatomy of the binary black hole recoil: A multipolar analysis. In: *Phys. Rev. D* 77 (2008), S. 044031. – arXiv:0707.0301

[266] Seidel, E. ; Suen, W.-M.: Towards a singularity-proof scheme in numerical relativity. In: *Phys. Rev. Lett.* 69 (1992), S. 1845–1848

[267] Shibata, M. ; Nakamura, T.: Evolution of three-dimensional gravitational waves: Harmonic slicing case. In: *Phys. Rev. D* 52 (1995), S. 5428–5444

[268] Shibata, M. ; Taniguchi, K.: Merger of black hole and neutron star in general relativity: Tidal disruption, torus mass, and gravitational waves. (2007). – arXiv:0711.1410 [gr-qc]

[269] Shibata, M. ; Taniguchi, K. ; Uryū, K.: Merger of binary neutron stars of unequal mass in full general relativity. In: *Phys. Rev. D* 68 (2003), S. 084020. – gr-qc/0310030

[270] Shoemaker, D. ; Smith, K. ; Sperhake, U. ; Laguna, P. ; Schnetter, E. ; Fiske, D.: Moving black holes via singularity excision. In: *Class. Quantum Grav.* 20 (2003), S. 3729–3743. – gr-qc/0301111

[271] Smarr, L.: *The structure of general relativity with a numerical illustration: The collision of two black holes*, University of Texas at Austin, Diss., 1975

[272] Smarr, L.: Gravitational Radiation From Distant Encounters And From Headon Collisions of Black Holes: The Zero Frequency Limit. In: *Phys. Rev. D* 15 (1977), S. 2069

[273] Smarr, L. ; Čadež, A. ; DeWitt, B. ; Eppley, K.: Collision of two black holes: Theoretical framework. In: *Phys. Rev. D* 14 (1976), S. 2443–2452

[274] Smarr, L. ; York, J. W. Jr.: Kinematical conditions in the construction of spacetime. In: *Phys. Rev. D* 17 (1978), S. 2529–2551

[275] Sopuerta, C. F. ; Yunes, N. ; Laguna, P.: Gravitational recoil from binary black hole mergers: The close limit approximation. In: *Phys. Rev. D* 74 (2006), S. 124010. – astro-ph/0608600

[276] Sopuerta, C. F. ; Yunes, N. ; Laguna, P.: Gravitational recoil velocities from eccentric binary black hole mergers. In: *Astrophys. J.* 656 (2007), S. L9–L12. – astro-ph/0611110

[277] Sperhake, U.: *Non-linear numerical Schemes in General Relativity*, School of Mathematics, University of Southampton, Diss., 2001

[278] Sperhake, U.: Binary black-hole evolutions of excision and puncture data. In: *Phys. Rev. D* 76 (2007), S. 104015. – gr-qc/0606079

[279] Sperhake, U. ; Berti, E. ; Cardoso, V. ; González, J. A. ; Brügmann, B. ; Ansorg, M.: Eccentric binary black-hole mergers: The transition from inspiral to plunge in general relativity. In: *Phys. Rev. D* 78 (2008), S. 064069. – arXiv:0710.3823 [gr-qc]

[280] Sperhake, U. ; Kelly, B. ; Laguna, P. ; Smith, K. L. ; Schnetter, E.: Black-hole head-on collisions and gravitational waves with fixed mesh-refinement and dynamic singularity excision. In: *Phys. Rev. D* 71 (2005), S. 124042. – gr-qc/0503071

[281] Sperhake, U. ; Smith, K. L. ; Kelly, B. ; Laguna, P. ; Shoemaker, D.: Impact of densitized lapse slicings on evolutions of a wobbling black hole. In: *Phys. Rev. D* 69 (2004), S. 024012. – gr-qc/0307015

[282] Szilágyi, B. ; Pollney, D. ; Rezzolla, L. ; Thornburg, J. ; Winicour, J.: An explicit harmonic code for black-hole evolution using excision. In: *Class. Quantum Grav.* 24 (2007), S. S275–S293. – gr-qc/0612150

[283] Tatsumi *et al.*, D.: Current status of Japanese detectors. In: *Class. Quantum Grav.* 24 (2007), S. S399. – arXiv:0704.2881 [gr-qc]

[284] Taylor, J. H. ; Weisberg, J. M.: Further experimental tests of relativistic gravity using the binary pulsar PSR 1913+16. In: *Astrophys. J.* 345 (1989), S. 434–450

[285] Thornburg, J.: Coordinates and boundary conditions for the general relativistic initial data problem. In: *Class. Quantum Grav.* 4 (1987), S. 1119–1131

[286] Thornburg, J.: A fast apparent-horizon finder for 3-dimensional Cartesian grids in numerical relativity. In: *Class. Quantum Grav.* 21 (2004), 21 January, S. 743–766. – gr-qc/0306056

[287] Thornburg, J. ; Diener, P. ; Pollney, D. ; Rezzolla, L. ; Schnetter, E. ; Seidel, E. ; Takahashi, R.: Are moving punctures equivalent to moving black holes? (2007). – gr-qc/0701038

[288] Thorne, K. S.: Multipole expansions of gravitational radiation. In: *Rev. Mod. Phys.* 52 (1980), S. 299–339

[289] Tichy, W. ; Brügmann, B.: Quasi-equilibrium binary black hole sequences for puncture data derived from helical Killing vector conditions. In: *Phys. Rev. D* 69 (2004), S. 024006. – gr-qc/0307027

[290] Tichy, W. ; Brügmann, B. ; Laguna, P.: Gauge conditions for binary black hole puncture data based on an approximate helical Killing vector. In: *Phys. Rev. D* 68 (2003), S. 064008. – gr-qc/0306020

[291] Vaishnav, B. ; Hinder, I. ; Herrmann, F. ; Shoemaker, D.: Matched Filtering of Numerical Relativity Templates of Spinning Binary Black Holes. In: *Phys. Rev. D* 76 (2007), S. 084020. – arXiv:0705.3829

[292] Volonteri, M. ; Haardt, F. ; Gultekin, K.: Compact massive objects in Virgo galaxies: the black hole population. (2007). – arXiv:0710.5770 [astro-ph]

[293] Volonteri, M. ; Haardt, F. ; Madau, P.: The Assembly and Merging History of Supermassive Black Holes in Hierarchical Models of Galaxy Formation. In: *Astrophys. J* 582 (2003), S. 559–573. – astro-ph/0207276

[294] Volonteri, M. ; Lodato, G. ; Natarajan, P.: The evolution of massive black hole seeds. In: *Mon. Not. R. Astron. Soc.* 383 (2008), S. 1079–1088. – arXiv:0709.0529 [astro-ph]

[295] Volonteri, M. ; Perna, R.: Dynamical evolutions of intermediate-mass black holes and their observational signatures in the nearby universe. In: *MNRAS* 358 (2005), S. 913–922. – astro-ph/0501345

[296] Washik, M. C. ; Healy, J. ; Herrmann, F. ; Hinder, I. ; Shoemaker, D. ; Laguna, P. ; Matzner, R. A.: Binary Black Hole Encounters, Gravitational Bursts and Maximum Final Spin. In: *Phys. Rev. Lett.* 101 (2008), S. 061102. – arXiv:0802.2520

[297] Winicour, J.: Characteristic Evolution and Matching. In: *Living Reviews in Relativity* 2005-10 (2005). – [Article in Online Journal] cited on 23 Feb 2001, http://relativity.livingreviews.org/Articles/lrr-2005-10/download/index.html

[298] Yo, H.-J. ; Baumgarte, T. W. ; Shapiro, S. L.: Improved numerical stability of stationary black hole evolution calculations. In: *Phys. Rev. D* 66 (2002), S. 084026. – gr-qc/0209066

[299] York, J. W. Jr.: Gravitational degrees of freedom and the initial-value problem. In: *Phys. Rev. Lett.* 26 (1971), S. 1656–1658

[300] York, J. W. Jr.: Role of conformal three-geometry in the dynamics of gravitation. In: *Phys. Rev. Lett.* 28 (1972), S. 1082–1085

[301] York, J. W. Jr.: Covariant decompositions of symmetric tensors in the theory of gravitation. In: *Ann. Inst. Henri Poincaré A* 21 (1974), S. 319–332

[302] York, J. W. Jr.: Kinematics and dynamics of general relativity. In: Smarr, L. (Hrsg.): *Sources of Gravitational Radiation*, Cambridge University Press, Cambridge, 1979, S. 83–126

[303] York, J. W. Jr.: The initial value problem and dynamics. In: Deruelle, T. N. & P. N. & Piran (Hrsg.): *Gravitational radiation*, North-Holland Publishing Company, 1983, S. 175–201

[304] York, J. W. Jr.: Conformal 'thin-sandwich' data for the initial-value problem of general relativity. In: *Phys. Rev. Lett.* 82 (1999), S. 1350–1353

[305] York, J. W. Jr. ; Piran, T.: The Initial Value Problem and Beyond. In: Matzner, R. A. (Hrsg.) ; Shepley, L. C. (Hrsg.): *Spacetime and Geometry*, 1982, S. 147–176

[306] Zerilli, F. J.: Tensor Harmonics in Canonical Form for Gravitational Radiation and Other Applications. In: *J. Math. Phys.* 11 (1970), S. 2203–2208

[307] Zlochower, Y. ; Baker, J. G. ; Campanelli, M. ; Lousto, C. O.: Accurate black hole evolutions by fourth-order numerical relativity. In: *Phys. Rev. D* 72 (2005), S. 024021. – gr-qc/0505055

Published Articles

Impact of densitized lapse slicings on evolutions of a wobbling black hole

Sperhake, U., K. L. Smith, B. Kelly, P. Laguna, & D. Shoemaker (2004)
Phys. Rev. D **69** 024012

Henceforth referred to as Paper 1

Black hole head-on collisions and gravitational waves with fixed mesh-refinement and dynamic singularity excision

Sperhake, U., B. Kelly, P. Laguna, K. L. Smith, & E. Schnetter (2005) *Phys. Rev. D* **71** 124042

Henceforth referred to as Paper 2

Binary black-hole evolutions of excision and puncture data

Sperhake, U. (2007)
Phys. Rev. D **76** 104015

Henceforth referred to as Paper 3

Calibration of Moving Puncture Simulations

Brügmann, B., J. A. González, M. D. Hannam, S. Husa, & U. Sperhake(2007)
Phys. Rev. D **77** 024027

Henceforth referred to as Paper 4

The maximum kick from non-spinning black-hole binary inspiral

González, J. A., U. Sperhake, B. Brügmann, M. D. Hannam, & S. Husa(2007)
Phys. Rev. Lett. **98** 091101

Henceforth referred to as Paper 5

Supermassive recoil velocities for binary black-hole mergers with anti-aligned spins

González, J. A., M. D. Hannam, U. Sperhake, B. Brügmann, & S. Husa
(2007)
Phys. Rev. Lett. **98** 231101

Henceforth referred to as Paper 6

Inspiral, merger and ringdown of unequal mass black hole binaries: a multipolar analysis

Berti, E., V. Cardoso, J. A. González, U. Sperhake, M. D. Hannam, S. Husa, & B. Brügmann (2007)
Phys. Rev. D **76** 064034

Henceforth referred to as Paper 7

Eccentric binary black-hole mergers: The transition from inspiral to plunge in general relativity

Sperhake, U., E. Berti, V. Cardoso, J. A. González, B. Bügmann, & M. Ansorg (2007)
submitted to *Phys. Rev. D*, arXiv:0710.3823 [gr-qc]

Henceforth referred to as Paper 8

Multipolar analysis of spinning binaries

Berti, E., V. Cardoso, J. A. González, U. Sperhake, & B. Brügmann
(2007)
accepted for publication in *Class. Quantum Grav.*, arXiv:0711.1097 [gr-qc]

Henceforth referred to as Paper 9

Erklärung

Ich erkläre hiermit, daß mir die Habilitationsordnung der Friedrich-Schiller-Universität Jena bekannt ist. Ferner erkläre ich, daß ich die vorliegende Arbeit ohne unzulässige Hilfe Dritter und ohne Benutzung anderer als der angegebenen Hilfsmittel angefertigt habe. Die aus anderen Quellen direkt oder indirekt übernommenen Daten und Konzepte sind unter Angabe der Quellen gekennzeichnet.

Die Mehrheit der vorgelegten wissenschaftlichen Veröffentlichungen wurde in Zusammenarbeit mit mehreren Koautoren erarbeitet. Den Veröffentlichungen liegen ferner insgesamt drei umfangreiche numerische Programme zur Simulation von Binärsystemen schwarzer Löcher zugrunde. Im folgenden stelle ich meinen Anteil an der Entwicklung dieser Programme, sowie meinen Anteil an den wissenschaftlichen Veröffentlichungen dar.

- Das Programm Maya wurde an der Penn State University von David Fiske, Bernard Kelly, Pablo Laguna, Erik Schnetter, Deirdre Shoemaker, Kenneth Smith und mir selbst entwickelt. Es basiert auf dem frei verfügbaren Programmpaketen Cactus und verwendet ferner die frei verfügbaren Programme Carpet von Erik Schnetter zur Gitterverfeinerung, und AHFinderDirect von Jonathan Thornburg zur Berechnung von scheinbaren Horizonten. Meine Beiträge zur Entwicklung des Codes sind die folgenden: die Korrektur des numerischen Zeitentwicklungssystems, wodurch stabile Simulationen möglich wurden; die Kombination des Maya Programms mit Carpet, welches Gitterverfeinerung in Maya möglich machten; die Implementierung von Eichbedingungen in Form der verdichteten lapse Funktion, sowie der Verwendung von Eichtrajektorien; die Entwicklung einer einfachen Methode zum Zweck der Lokalisierung schwarzer Löcher innerhalb des numerischen Gitters; zusammen mit Bernard Kelly das Erstellen von Programmodulen zur Extraktion von Gravitationswellen in Form der Störungsrechnung nach Zerilli und Moncrief, sowie in Form der Newman-Penrose Skalare. Die Beiträge meiner Mitarbeiter beinhalten die Erstellung des Gerüstes des Kodes, sowie die Implementierung der BSSN Entwicklungsgleichungen, der "excision" Methode der Singularität, diverser Anfangsdaten sowie Methoden der zwei- und dreidimensionalen Visualisierung.

- Das Programm Bam ist im wesentlichen von Bernd Brügmann entwickelt worden. Meine Beiträge zu diesem Programm bestehen in der Korrektur und Verfeinerung der Module zur Extraktion von Gravitationswellen sowie der Berechnung scheinbarer Horizonte.

- Das Programm Lean basiert auf dem frei verfügbaren Paket Cactus und verwendet Carpet zur Gitterverfeinerung, AHFinderDirect zur Berechnung scheinbarer Horizonte, sowie das Paket TwoPunctures von Marcus Ansorg zur Berechnung von Anfangsdaten des Punkturtyps. Von der Verwendung dieser freien Programmpakete abgesehen wurde der Lean Kode vollständig von mir ohne Mithilfe weiterer Personen erstellt.

- Die dem Artikel “Paper 1” zugrundeliegende Idee, eine verdichtete Version der lapse Funktion zu verwenden geht auf Pablo Laguna zurück. Die numerischen Simulationen, sowie deren Analyse und die graphische Gestaltung der Ergebnisse in der Veröffentlichung wurden von mir duchgeführt.

- Die numerischen Simulationen, die letztendlich in dem Artikel “Paper 2” dargestellt wurden, sowie deren Auswertung sind von mir durchgeführt worden. Der Arbeit liegen jedoch eine größere Anzahl weiterer Testsimulationen zugrunde, die von Bernard Kelly, Kenneth Smith und mir durchgeführt wurden.

- Die Veröffentlichung “Paper 4” beinhaltet zahlreiche numerische Simulationen einzelner schwarzer Löcher, sowie Binärsysteme. Mein Beitrag zu dieser Arbeit liegt in der schon erwähnten Extraktion von Gravitationswellen zusammen mit José González, sowie der Durchführung einiger der Simulationen, die es uns ermöglichten, Parameter für eine saubere Kovergenz zu bestimmen. Ferner erstellte ich die Ergebnisses des Lean Kodes, die zum Vergleich der Ergebnisse verwendet wurden. Die weiteren Simulationen und deren Analyse wurde größtenteils von Bernd Brügmann, Mark Hannam und Sascha Husa durchgeführt.

- Der Artikel “Paper 5” beruht auf einer großen Anzahl an Simulationen von Binärsystemen mit ungleichen Massenverhältnissen. Diese Simulationen, sowie eine große Anzahl an Testläufen zwecks Konvergenzbestimmung wurden von José González und mir durchgeführt. Die Auswertung hinsichtlich abgestrahlter Gravitationswellen, sowie des Rückstoßeffektes wurden unter Beteiligung aller Autoren ausgeführt. Auf die Bedeutung der Berechnung des Rückstoßeffektes für die Astrophysik hat insbesondere José González hingewiesen. Diese numerischen Ergebnisse sind auch Grundlage der multipolaren Analyse des Artikels “Paper 6”. Die Analyse wurde größtenteils von Emanuele Berti, Vitor Cardoso, José González und mir durchgeführt. Die Idee dieser Analyse geht auf eine Initiative von Emanuele Berti und Vitor Cardoso zurück, die auch den Vergleich der numerischen Daten mit Post-Newton'schen Ergebnissen und den quasi-normalen Oszillationen des verschmolzenen Loches durchführten. Die Berechnung des gravitativen Pola-risationen h_+, $h_\times$, sowie der Phasen und Frequenzen des numerischen Gravitationswellensignals, die dem Vergleich dienten, wurde von mir vorgenommen.

- Die Simulation zur Berechnung des Rückstoßeffektes in Artikel “Paper 7” wurde zunächst von mir mit Lean vorgenommen. Die Idee enstammte einer Veröffentlichung der Forschungsgruppe der Universität in Rochester, NY. Angesichts der stark überraschenden Ergebnisses haben Bernd Brügmann und José González eine Kontrolle des Ergebnisses unter Verwendung des unabhängigen Bam Kodes vorgenommen. Die Konvergenzanalyse und daraus resultierende Abschätzung der Genauigkeit des Ergebnisses wurde von mir vorgenommen.

- Artikel “Paper 8” präsentiert die Analyse einer Sequenz von Simulationen einspirallierender Binärsysteme mit unterschiedlicher Exzentrizität dar. Die Simulationen wurden von mir unter Verwendung des LEAN codes vorgenommen. Selbes gilt für die unmittelbare Analyse der Simulationen, d. h. die Berechnung der Gravitationswellenmoden und ihrer Phasen und Frequenzen. Die weitergehende Analyse wurde weitestgehend von Emanuele Berti und Vitor Cardoso durchgeführt. Hierzu gehören insbesondere die Berechnung der Polarisation, sowie die Beobachtung des kritischen Bahndrehimpulswertes. Die analytischen Schätzungen der Exzentrizität wurden von Emanuele Berti und mir unter Verwendung der Literatur erstellt.

- Dem Artikel “Paper 9” liegen die bereits in Paper 5 und 6 analysierten Simulationen zugrunde. Diese wurden mit neuen, von mir berechneten Simulationen von Binärsystemen mit Spin verglichen. Die multipolare Analyse der Daten wurde größtenteils von Emanuele Berti, Vitor Cardoso und mir vorgenommen. Die Idee, in der Verschmelzung ein nicht-rotierendes Schwarzschild Loch zu generieren entstammt einer Arbeit von Buonanno, Kidder und Lehner. Die Analyse der Ergebnisse vor dem Hintergrund Post-Newton'scher Vorhersagen wurde von Emanuele Berti und Vitor Cardoso duchgeführt.

Weitere Personen waren an der inhaltlich-materiellen Erstellung der Arbeit nicht beteiligt. Insbesondere habe ich hierfür nicht entgeltliche Hilfe von Vermittlungsbzw. Beratungsdiensten in Anspruch genommen. Niemand hat von mir unmittelbar oder mittelbar geldwertige Leistungen für Arbeiten erhalten, die im Zusammenhang mit dem Inhalt der vorgelegten Arbeit stehen.

Die Arbeit wurde bisher weder im In- noch Ausland in gleicher oder ähnlicher Form einer anderen Prüfungsbehörde vorgelegt.

Ich versichere, daß ich nach bestem Wissen die reine Wahrheit gesagt und nichts verschwiegen habe.

Jena, den 13.April 2008

Ulrich Sperhake

Lebenslauf

	Sperhake, Ulrich
14. April 1968	Buchholz i. d. Nordheide
	ledig
Aug 1974 - Jun 1978	Grundschule, Wiesenschule Buchholz
Aug 1978 - Mai 1987	Albert-Einstein-Gymnasium Buchholz
1987	Abitur
Okt 1991 - Jun 1997	Physikstudium and der Universität Hamburg
25.7.1997	Hochschulabschluß, Physik Diplom
Aug 1997 - Sep 1997	Wiss. Mitarbeiter, Sternwarte Bergedorf
Okt 1997 - Sep 1998	Wiss. Mitarbeiter, Insitut für Astronomie und Astrophysik, Christian-Albrechts-Universität Kiel
Okt 1998 - Okt 2001	Doktorand an der “School of Mathematics”, Universität Southampton
17.12.2001	Promotion an der Universität Southampton, “Non-linear numerical Schemes in General Relativity”
Nov 2001 - Aug 2002	Post-doc, Universität Thessaloniki
Sep 2002 - Aug 2005	Post-doc, Penn State University
Sep 2005 -	Post-doc, Friedrich-Schiller Universität Jena